**Non-Linear Strain Energy Formulation of a Generalized Bisymmetric Spatial Beam for Flexure Mechanism Analysis**

**Authors**

Shiladitya Sen[1] and Shorya Awtar

Precision Systems Design Lab

Mechanical Engineering, University of Michigan

2350 Hayward Street, Ann Arbor, MI 48109

Email: awtar@umich.edu, Phone: (734) 615-0285, Fax: (734) 647-3170

**Abstract**

Analytical load-displacement relations for flexure mechanisms, formulated by integrating the individual analytical models of their building-blocks (i.e. flexure elements), help in understanding the constraint characteristics of the whole mechanism. In deriving such analytical relations for flexure mechanisms, energy based approaches generally offer lower mathematical complexity, compared to Newtonian methods, by reducing the number of unknowns – specifically, the internal loads. To facilitate such energy based approaches, a closed-form non-linear strain energy expression for a generalized bisymmetric spatial beam flexure is presented in this paper. The strain energy, expressed in terms of the end-displacement of the beam, considers geometric nonlinearities for intermediate deformations, enabling the analysis of flexure mechanisms over a finite range of motion. The generalizations include changes in the initial orientation and shape of the beam flexure due to potential misalignment or manufacturing. The effectiveness of this approach is illustrated via the analysis of a multi-legged table flexure mechanism. The resulting analytical model is shown to be accurate using non-linear finite elements analysis, within a load and displacement range of interest.

[1] Corresponding Author

**Keywords:** Spatial Beam Flexure, Geometric Non-linearities, Strain Energy, Flexure Mechanisms, Beam Constraint Model, Multi-legged Table Flexure

## 1. INTRODUCTION AND BACKGROUND

Flexure mechanisms rely on the elastic deformation of flexure elements to provide small but smooth and precise motions, and are important in machine design at all scales [1, 2].

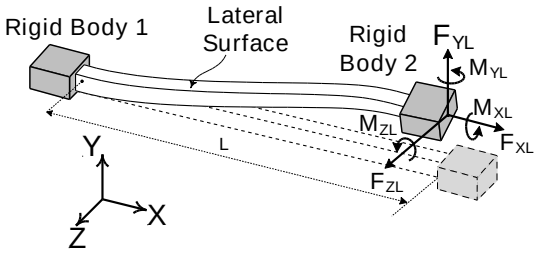


*Figure 1: Spatial Beam Flexure, Undeformed and Deformed Configurations*

One of the commonly used flexure elements is a spatial beam, which exhibits relatively high stiffness along its centroidal axis in comparison to displacements in the transverse direction and torsion. Figure 1 illustrates an initially straight slender prismatic spatial beam of length $L$ that connects rigid bodies (1) and (2). An analytical model of the spatial beam, which we refer to as the spatial beam constraint model (SBCM), relates the six independent end-displacements to the six independent end-loads over an intermediate translational and angular displacement range of $0.1L$ and 0.1 radians, respectively, was formulated in reference [3]. The primary advantage of SBCM over other existing models of spatial beams [4, 5] is its generality in the application of loads and displacements and its relatively simpler mathematical form. Here the relative displacements, i.e. translations and angular rotations of rigid body 2 with respect to rigid body 1, are represented by $\{U_{XL}, U_{YL}, \text{ and } U_{ZL}\}$ and $\{\Theta_{XdL}, -U'_{ZL}, U'_{YL}\}$, respectively. The twist $\Theta_{XdL}$ is measured about the tangent to the centroidal axis of the deformed beam. Furthermore, $-U'_{ZL}$ and $U'_{YL}$, which are the slopes of the projection of the beam on XZ and XY planes respectively, are often approximated as angles $\Theta_{YL}$ and $\Theta_{ZL}$ for small values of the order of 0.1. The six independent end-loads are $\{\boldsymbol{F}_{XL}, \boldsymbol{F}_{YL}, \boldsymbol{F}_{ZL}, \boldsymbol{M}_{XL}, \boldsymbol{M}_{YL} \text{ and } \boldsymbol{M}_{ZL}\}$ as shown in Figure 1. The '$L$' in the subscript of the loads and displacement variable indicate that the values are measured at the end of the beam i.e. at $X=L$. The term 'load' is used here in a generalized sense, indicating both forces and moments.

The SBCM is applicable to slender prismatic beams with 'bisymmetric cross-section' which is defined in this paper as a cross-section for which area moments of inertia $I_{YY}$ and $I_{ZZ}$ are equal and $I_{YZ}$ is zero. The two equal area moments of inertia $I_{YY}$ and $I_{ZZ}$ are represented simply as $I$. This restriction makes a closed-form solution of the beam

governing equations possible, as shown later. Examples of such bisymmetric cross-sections are circles and even-sided regular polygons. The key contribution of SBCM is that it captures geometric nonlinearities associated with arc-length conservation and coupling between XY and XZ bending planes due to torsion in a closed-form manner without sacrificing accuracy or generality in the loading or displacement conditions [3]. Additionally, a compatible expression of strain energy in terms of the end-displacements and loads $\boldsymbol{F_{XL}}$ and $\boldsymbol{M_{XL}}$ was provided. This enables the use of energy methods such as principle of virtual work [6], as an alternative to Newtonian methods for the analysis of flexure mechanisms. With these attributes, it was shown that SBCM is able to capture the constraint characteristics of flexure mechanisms in terms of stiffness values and error motion with 95% accuracy over a range of 0.1L and 0.1 radians for translational and angular displacements.

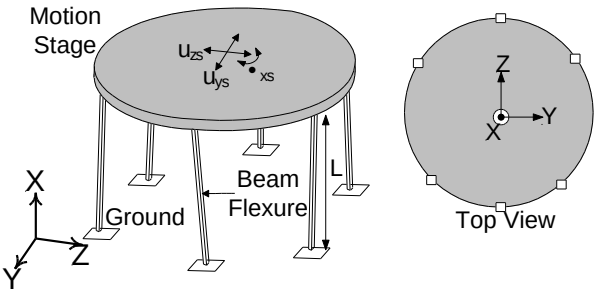


*Figure 2: A 3-DoF Spatial Flexure Mechanism*

In order to improve the versatility of the SBCM, this paper captures the effect of angular misalignments and variable cross-sections in spatial bisymmetric beams. These geometric generalizations are reflected in a new closed-form non-linear strain energy expression for spatial beams. The resulting generalized SBCM is used to analyze a spatial table flexure with multiple legs, shown in Figure 2, using energy methods. It is assumed that the multiple legs in this table flexure are not perfectly parallel due to manufacturing defects or intentional design.

In practice, the multi-legged table flexure mechanism is used to provide relatively high stiffness against out-of-plane translational displacements along X and out-of-plane rotational displacements about Y and Z while allowing in-plane translation motions along Y and Z and in-plane rotation about X. A 4-legged version of this mechanism has been used make precision positioning stages [7] while a 3-legged version with tilted beams is used to make a compliant assembly device [8], a vibratory bowl feeder [9], and a minimally invasive surgical tool [10]. Furthermore, this spatial mechanism provides alternative designs [11] to leaf flexure based planar positioning stage [12].

Although a linear model of the spatial beam flexure [13] can be used to derive basic insight, a nonlinear analysis technique is desirable in order to capture geometric effects. Nonlinear analysis may be numerical in nature

like FEA or closed-form. In this article we explore a closed-form nonlinear analysis methodology. Nonlinear closed formed analysis of the multi-legged table flexure mechanism, comprising *n* spatial beam flexures connected to a rigid motion stage, using Newtonian methods is difficult because it requires solving 12n+6 unknowns (each leg contributes 6 internal end-loads and 6 internal end-displacements while the motion stage contributes 6 displacements) from 12n+6 simultaneous equations (each leg contributes 6 load-displacement relations between its respective end-loads and end-displacements and 6 geometric compatibility relations between its end-displacements and the motion stage displacements, and the motion stage contributes 6 load-equilibrium relations). Although Hao presented such an analytical formulation for a three-legged table with vertical beam flexures [14], the complexity of the derivation showed that a similar analysis for four or more legged table would be difficult.

The mathematical complexity increases even more for a multi-legged table flexure mechanism with non-parallel spatial beam flexures. This is because the local co-ordinate frame for each spatial beam flexure is different from global co-ordinate frame of the multi-legged table flexure mechanism. Although, often a numerical approach such as Finite Element Analysis (FEA) is used to overcome the complexity, as a tradeoff, parametric design insights that help us improve the design become non-obvious.

Accordingly, this paper recognizes that this problem may be solved more tractably using an energy based approach and focuses on finding a closed form model for multi-legged (arbitrary n) table flexure with non-parallel legs. To this end, section 2 derives the SBCM of bisymmetric spatial beam flexure with a small but otherwise arbitrary tilt. By including the effect of tilt in the strain energy expression of SBCM itself, there is no longer a need for co-ordinate transformation as the displacement variables of all the spatial beam flexures can be defined in the global co-ordinate system. This also simplifies the mathematical procedure considerably and allows us to easily model a highly generalized multi-legged table flexure mechanism with non-parallel spatial beam flexures in a closed-form manner.

In order to show the validity of the form of SBCM for spatial beam flexures with generalized shape, this paper also discusses the fundamental relations between the beam characteristic coefficients $[H_1]$-$[H_7]$ in section 3. This analysis shows that the pertinent effects associated with the geometric nonlinearities for a bisymmetric spatial beam flexure with varying cross-section, can be captured in SBCM by only changing the beam characteristic coefficients $[H_1]$-$[H_7]$. Furthermore, this discussion also illustrates the formulation of the entire SBCM of such a beam flexure using the solution of the linearly coupled differential equations associated with bending in the XY and XZ

plane only. This implies the nonlinear differential equations associated with axial extension, torsion and strain energy need not be solved for determination of SBCM.

Section 4 uses the generalized SBCM that captures tilt as well as shape variation to model a multi-legged table flexure mechanism with n identical legs with small but otherwise arbitrary tilt. For validation, the load-displacement results of a 3 legged table, composed of 3 prismatic slender spatial beams, are compared with FEA. Finally, section 5 provides a conclusion this paper with a brief discussion on contributions and future work.

## 2. STRAIN ENERGY OF A BISYMMETRIC SPATIAL BEAM WITH ARBITRARY TILT

A slender beam with equal thickness that is not perfectly parallel with the X-axis of a global reference co-ordinate frame X-Y-Z, due to manufacturing/assembly defects or intentional design, is shown in Figure 3. The orientation of the unloaded undeformed beam may be described by rotating a beam that is initially aligned with the X-axis, through an Euler rotation sequence of $\beta$ about the Y axis and $\gamma$ about the rotated Z axis. The resulting co-ordinate frame is called $X_T$-$Y_T$-$Z_T$ where $Y_TZ_T$ represents the cross-sectional plane which $X_T$ represents the centroidal axis of the tilted beam.

Next, we express the deformation of the beam in terms of displacement variables defined in the X-Y-Z co-ordinate frame. The deformation of any cross-section perpendicular to the undeformed centroidal axis is determined to be a rigid body translation and rotation followed by an out of plane warping. This deformation assumption is based on (i) the Euler Bernoulli assumption which ignores shear effects due to shear forces $\boldsymbol{F_{YL}}$ and $\boldsymbol{F_{ZL}}$ in comparison to bending for slender beams with thickness/length ratio less than 1/20 [15], and (ii) St. Venant solution of slender prismatic beam that shows in-plane distortion to be absent. A more detailed analysis of the assumptions can be found the analysis of non-tilted uniform bisymmetric spatial beam in reference [3]. The translation of the centroidal point P of any cross-section perpendicular to the undeformed centroidal axis to its deformed position P' is represented by $U_X$, $U_Y$ and $U_Z$ along the X, Y and Z axes, respectively, as shown in Figure 3(a). The rigid body rotation of the cross-section containing P is defined by three Euler rotations $-\varphi-\beta$ about the Y axis followed by $\psi+\gamma$ about the rotated Z axis followed by $\Theta_{Xd}$ about the rotated X axis as shown in Figure 3(b). Let the resulting deformed co-ordinate frame be called $X_d$-$Y_d$-$Z_d$ in which $X_d$ axis is defined along the tangent to the deformed centroidal axis while $Y_dZ_d$ forms the deformed cross-sectional plane prior to warping. Finally, in addition to rigid body translation and rotation, the warping of the cross-section causes small displacements along the $X_d$ axis.

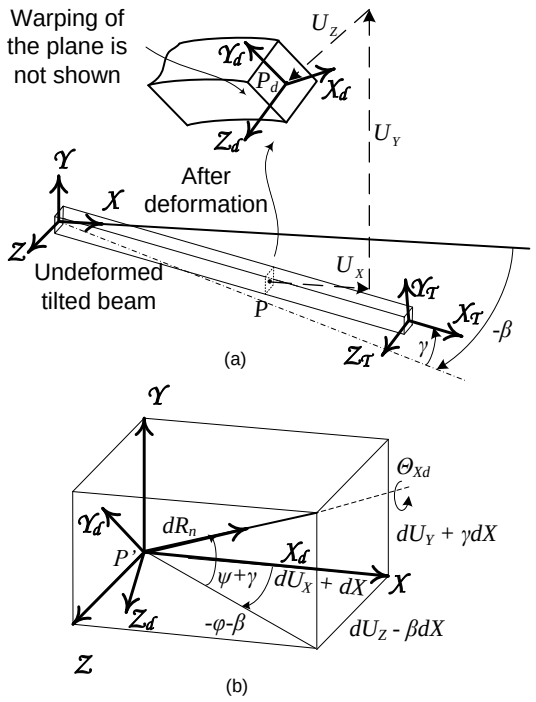


*Figure 3: (a) Tilted Spatial Beam deformation (b) Relating the orientation of the $X_T$-$Y_T$-$Z_T$ co-ordinate frame and $X_d$-$Y_d$-$Z_d$ co-ordinate frame*

Using this beam deformation, the strain at any general point before deformation with coordinate position (X, Y, Z) may be defined using Green's strain measure.

$$d\vec{R}_d \bullet d\vec{R}_d - d\vec{R}_0 \bullet d\vec{R}_0 = 2\begin{Bmatrix} dX \\ dY \\ dZ \end{Bmatrix}^T \begin{bmatrix} \varepsilon_{XX} & \varepsilon_{XY} & \varepsilon_{XZ} \\ \varepsilon_{YX} & \varepsilon_{YY} & \varepsilon_{YZ} \\ \varepsilon_{ZX} & \varepsilon_{ZY} & \varepsilon_{ZZ} \end{bmatrix} \begin{Bmatrix} dX \\ dY \\ dZ \end{Bmatrix} \quad (1)$$

Here $\vec{R}_0$ is the position vector of this point before deformation and equal to $\{X \quad Y+\gamma X \quad Z-\beta X\}^T$. Position vector $\vec{R}_d$ represents the position of this point after deformation and is calculated by vectorially adding the relative displacement of P' with respect to P, the relative displacement of this point with respect to P' in the deformed configuration and displacement due to warping at his point which is along $X_d$. The transformation matrix relating X-Y-Z co-ordinate frame and $X_d$-$Y_d$-$Z_d$ co-ordinate frame is essential in determining $\vec{R}_d$ and can be expressed using derivatives of $U_X$, $U_Y$, $U_Z$ and $\Theta_{Xd}$ using Figure 3(b). The final expression for non-linear strain, approximated to the second order, may be derived using Eq.(2) to be:

$$\varepsilon_{XX} \approx U_X' + \gamma U_Y' - \beta U_Z' + \frac{1}{2}U_Y'^2 + \frac{1}{2}U_Z'^2 - Y\kappa_{Zd} + Z\kappa_{Yd} + \frac{1}{2}\kappa_{Xd}{}^2\left(Y^2 + Z^2\right) \tag{2}$$

$$\gamma_{XY} \approx \kappa_{Xd}\left[Y - Y_W\right] \qquad \text{where } Y_W \triangleq \frac{d\lambda}{dZ} \tag{3}$$

$$\gamma_{XZ} \approx \kappa_{Xd}\left[Z - Z_W\right] \qquad \text{where } Z_W \triangleq \frac{d\lambda}{dY} \tag{4}$$

The rate of twist angle, $\kappa_{Xd}$, and bending curvatures $\kappa_{Yd}$ and $\kappa_{Zd}$ can be expressed, to the second order approximation, as follows:

$$\begin{aligned} \kappa_{Xd} &\approx \Theta_{Xd}' - U_Z''\left(U_Y' + \gamma\right); \\ \kappa_{Yd} &\approx \sin\left(\Theta_{Xd}\right)U_Y'' - \cos\left(\Theta_{Xd}\right)U_Z''; \\ \kappa_{Zd} &\approx \cos\left(\Theta_{Xd}\right)U_Y'' + \sin\left(\Theta_{Xd}\right)U_Z'' \end{aligned} \tag{5}$$

The out-of-plane warping along $X_d$ is estimated to be $\lambda \cdot \kappa_{Xd}$ [16], where $\lambda$ is a warping function dependent on only the local cross-sectional coordinates $Y_d$ and $Z_d$ and independent of coordinate $X$.

Using the strain expressions in Eqs.(2) -(4), the strain energy for the initially tilted spatial beam flexure is expressed below by assuming linear material properties. It should be noted that for a slender beam, stresses along Y and Z axes may be approximated to be zero and hence strains $\varepsilon_{YY}$ and $\varepsilon_{ZZ}$ do not appear in the calculation of the strain energy.

$$V = \frac{E}{2}\int_{vol}\varepsilon_{xx}^2\,dAdX + \frac{G}{2}\int_{vol}\left(\gamma_{xy}^2 + \gamma_{xz}^2\right)dAdX \tag{6}$$

Once the total strain energy for the spatial beam has been obtained, the Principle of Virtual Work (PVW) [6] may be applied to generate the beam differential equations and boundary conditions. According to the PVW, the virtual work done by external forces over a set of geometrically compatible but otherwise arbitrary 'virtual' displacements is equal to the change in the strain energy due to these 'virtual' displacements:

$$\delta W = \delta V \tag{7}$$

Using PVW, the beam governing differential equations and natural boundary conditions is derived using a similar procedure as described in reference [3]. Also, at this stage we introduce that following normalization scheme:

$$\boldsymbol{m}_{z1} \triangleq \frac{\boldsymbol{M}_{ZL} L}{EI}, \boldsymbol{m}_{y1} \triangleq \frac{\boldsymbol{M}_{YL} L}{EI}, \boldsymbol{m}_{xd1} \triangleq \frac{\boldsymbol{M}_{XdL} L}{EI}, \boldsymbol{f}_{z1} \triangleq \frac{\boldsymbol{F}_{ZL} L^2}{EI},$$
$$\boldsymbol{f}_{y1} \triangleq \frac{\boldsymbol{F}_{YL} L^2}{EI}, \boldsymbol{f}_{x1} \triangleq \frac{\boldsymbol{F}_{XL} L^2}{EI}, \nu \triangleq \frac{VL}{EI}, \; u_y \triangleq \frac{U_Y}{L}, \; u_z \triangleq \frac{U_Z}{L}, \tag{8}$$
$$u_{y1} \triangleq \frac{U_{YL}}{L}, \; u_{z1} \triangleq \frac{U_{ZL}}{L}, \; x \triangleq \frac{X}{L}, \; \theta_{xd} \triangleq \Theta_{Xd}, \; \theta_{xd1} \triangleq \Theta_{XdL}$$

The normalized beam governing differential equations are

$$\begin{aligned}
&u_y^{iv} - \boldsymbol{f}_{x1} u_Y'' + \boldsymbol{m}_{xd1} u_z''' = 0 \\
&u_z^{iv} - \boldsymbol{f}_{x1} u_Z'' - \boldsymbol{m}_{xd1} u_y''' = 0 \\
&u_x' + \gamma u_y' - \beta u_z' + \frac{1}{2} u_y'^2 + \frac{1}{2} u_z'^2 = \frac{\boldsymbol{f}_{x1}}{k_x} - \frac{\boldsymbol{m}_{xd1}^2}{k_x k_\theta^2} \\
&\left\{ \theta_{xd}' - u_z'' \left( u_y' + \gamma \right) \right\} = \frac{\boldsymbol{m}_{xd1}}{k_\theta} - \frac{2 \boldsymbol{m}_{xd1} \boldsymbol{f}_{x1}}{k_x k_\theta^2}
\end{aligned} \tag{9}$$

The normalized natural boundary conditions are

$$\begin{aligned}
\boldsymbol{f}_{y1} &= \boldsymbol{f}_{x1} u_{y1}' - u_{y1}''' - \boldsymbol{m}_{xd1} u_{z1}'' \\
\boldsymbol{f}_{z1} &= \boldsymbol{f}_{x1} u_{z1}' - u_{z1}''' + \boldsymbol{m}_{xd1} u_{y1}'' \\
\boldsymbol{m}_{y1} &= -u_{z1}'' + \boldsymbol{m}_{xd1} u_{y1}' \\
\boldsymbol{m}_{z1} &= u_{y1}'' + \boldsymbol{m}_{xd1} u_{z1}'
\end{aligned} \tag{10}$$

where, $k_x \triangleq \frac{12 L^2}{T_Y^2}$, $k_\theta \triangleq \frac{GJ}{EI}$,

$\boldsymbol{m}_{xd1} \triangleq \boldsymbol{m}_{x1} + \left( u_y' + \gamma \right) \boldsymbol{m}_{y1} + \left( u_{z1}' - \beta \right) \boldsymbol{m}_{z1}$

All the loads and displacements are normalized per the following scheme to make the equations and results compact:

Here $E$ is the elastic modulus, while $L$ is the length of the projection of the spatial beam flexure along the X axis. $T_Y$ is the thickness of the beam along Y. Since $u_{y1}' + \gamma$ and $u_{z1}' - \beta$ are approximately equal to rotations about Z and Y axes respectively, $\boldsymbol{m}_{xd1}$ is simply the normalized equivalent torsional moment expressed along the deformed centroidal axis at the free end of the beam. The normalized geometric boundary conditions are:

$$\begin{aligned}
&u_y(0) = 0 \; ; \; u_z(0) = 0 \; ; \; u_y'(0) = 0 \; ; \; u_z'(0) = 0 \; ; \\
&u_x(0) = 0 \; ; \; \theta_{xd}(0) = 0 \; ; \; u_y(1) \triangleq u_{y1}; \; u_z(1) \triangleq u_{z1}; \\
&u_y'(1) \triangleq u_{y1}'; \; u_z'(1) \triangleq u_{z1}'; \; u_x(1) \triangleq u_{x1} \; ; \; \theta_{xd}(1) \triangleq \theta_{xd1}
\end{aligned}$$

It should be noted that at this stage if $\beta$ and $\gamma$ are set to zero, then the differential equations became same as that for a non-tilted beam [3] as expected. The strain energy expression can be also stated compactly as follows after normalization:

$$v = \frac{1}{2}\int_0^1 \left(u_y''^2 + u_z''^2\right) dx + \frac{\boldsymbol{m}_{xd1}^2}{2k_\theta} + \frac{\boldsymbol{f}_{x1}^2}{2k_x} - \frac{2\boldsymbol{m}_{xd1}^2 \boldsymbol{f}_{x1}}{k_x k_\theta^2} \tag{11}$$

Capturing the various non-linear coupling effects renders the governing equations of extension and torsion non-linear. However the bending equations are still linear albeit coupled in $u_y$ and $u_z$. This allows the first two equations of Eq.(9), along with associated boundary conditions, to be solved using linear algebra techniques and then the results can be substituted in last two equations of Eq. (9) to solve for $u_x$ and $\theta_{xd}$, which provide the two geometric constraint conditions. The results may also be substituted in the strain energy term.

To express this result in a form that is mathematically concise and provides insight into the effects of geometric non-linearities that are relevant to constraint characterization, we carry out a Taylor series expansion of the solution of $\boldsymbol{f}_{y1}$, $\boldsymbol{f}_{z1}$, $\boldsymbol{m}_{y1}$, and $\boldsymbol{m}_{z1}$ in terms of the axial and torsional loads, $\boldsymbol{f}_{x1}$ and $\boldsymbol{m}_{xd1}$ and drop third and higher power terms. Since the coefficients of $\boldsymbol{f}_{x1}$ and $\boldsymbol{m}_{xd1}$ diminish quickly with increasing powers, this truncation results in less 1% error in the displacement and load range of interest. Similarly Taylor series expansion of the solutions of $\boldsymbol{u}_{x1}$ and $\boldsymbol{\theta}_{xd1}$ in terms of $\boldsymbol{f}_{x1}$ and $\boldsymbol{m}_{xd1}$ are also carried out and second and higher power terms are dropped. Error due to truncation in this case is less than 5% for the normalized $\boldsymbol{f}_{x1}$ and $\boldsymbol{m}_{xd1}$ values less than 5. The SBCM for tilted spatial beam flexure is

$$\begin{aligned}
&\left\{\boldsymbol{f}_{y1} \quad \boldsymbol{m}_{z1} \quad \boldsymbol{f}_{z1} \quad \boldsymbol{m}_{y1}\right\}^T = [H_1]\left\{u_{y1} \quad u'_{y1} \quad u_{z1} \quad -u'_{z1}\right\}^T \\
&+\boldsymbol{m}_{xd1}\left\{0 \quad -\beta \quad 0 \quad \gamma\right\}^T + \boldsymbol{f}_{x1}\left\{\gamma \quad 0 \quad -\beta \quad 0\right\}^T \\
&-\left(2\boldsymbol{f}_{x1}[H_2] + \boldsymbol{m}_{xd1}\left(2[H_3] + [H_7]\right)\right)\left\{u_{y1} \quad u'_{y1} \quad u_{z1} \quad -u'_{z1}\right\}^T \\
&-\left(\boldsymbol{f}_{x1}^2[H_4] + \boldsymbol{m}_{xd1}\boldsymbol{f}_{x1}[H_5] + \boldsymbol{m}_{xd1}^2[H_6]\right)\left\{u_{y1} \quad u'_{y1} \quad u_{z1} \quad -u'_{z1}\right\}^T
\end{aligned} \tag{12}$$

$$\begin{aligned}
&u_{x1} = \frac{\boldsymbol{f}_{x1}}{k_x} - \frac{\boldsymbol{m}_{xd1}^2}{k_\theta^2 k_x} - \gamma u_{y1} + \beta u_{z1} \\
&+\left\{u_{y1} \quad u'_{y1} \quad u_{z1} \quad -u'_{z1}\right\}[H_2]\left\{u_{y1} \quad u'_{y1} \quad u_{z1} \quad -u'_{z1}\right\}^T \\
&+\boldsymbol{f}_{x1}\left\{u_{y1} \quad u'_{y1} \quad u_{z1} \quad -u'_{z1}\right\}[H_4]\left\{u_{y1} \quad u'_{y1} \quad u_{z1} \quad -u'_{z1}\right\}^T \\
&+\frac{1}{2}\boldsymbol{m}_{xd1}\left\{u_{y1} \quad u'_{y1} \quad u_{z1} \quad -u'_{z1}\right\}[H_5]\left\{u_{y1} \quad u'_{y1} \quad u_{z1} \quad -u'_{z1}\right\}^T
\end{aligned} \tag{13}$$

$$\theta_{xd1} = \frac{\boldsymbol{m}_{xd1}}{k_\theta} - \frac{2\boldsymbol{m}_{xd1}\boldsymbol{f}_{x1}}{k_x k_\theta^2} + u'_{z1}\gamma + \begin{Bmatrix} u_{y1} \\ u'_{y1} \\ u_{z1} \\ -u'_{z1} \end{Bmatrix}^T [H_3] \begin{Bmatrix} u_{y1} \\ u'_{y1} \\ u_{z1} \\ -u'_{z1} \end{Bmatrix}$$
$$+ \begin{Bmatrix} u_{y1} \\ u'_{y1} \\ u_{z1} \\ -u'_{z1} \end{Bmatrix}^T \left( \boldsymbol{m}_{xd1}[H_6] + \frac{1}{2}\boldsymbol{f}_{x1}[H_5] \right) \begin{Bmatrix} u_{y1} \\ u'_{y1} \\ u_{z1} \\ -u'_{z1} \end{Bmatrix} \tag{14}$$

$$v = \frac{\boldsymbol{m}_{xd1}^2}{2k_\theta} + \frac{\boldsymbol{f}_{x1}^2}{2k_x} - \frac{2\boldsymbol{m}_{xd1}^2\boldsymbol{f}_{x1}}{k_x k_\theta^2}$$
$$+ \frac{1}{2} \begin{Bmatrix} u_{y1} \\ u'_{y1} \\ u_{z1} \\ -u'_{z1} \end{Bmatrix}^T \left( \begin{matrix} [H_1] + \boldsymbol{f}_{x1}^2[H_4] + \\ \boldsymbol{m}_{xd1}\boldsymbol{f}_{x1}[H_5] + \boldsymbol{m}_{xd1}^2[H_6] \end{matrix} \right) \begin{Bmatrix} u_{y1} \\ u'_{y1} \\ u_{z1} \\ -u'_{z1} \end{Bmatrix} \tag{15}$$

where

$$[H_1] \triangleq \begin{bmatrix} 12 & -6 & 0 & 0 \\ -6 & 4 & 0 & 0 \\ 0 & 0 & 12 & 6 \\ 0 & 0 & 6 & 4 \end{bmatrix}, [H_2] \triangleq -\begin{bmatrix} \frac{3}{5} & -\frac{1}{20} & 0 & 0 \\ -\frac{1}{20} & \frac{1}{15} & 0 & 0 \\ 0 & 0 & \frac{3}{5} & \frac{1}{20} \\ 0 & 0 & \frac{1}{20} & \frac{1}{15} \end{bmatrix} [H_4] \triangleq \begin{bmatrix} \frac{1}{700} & -\frac{1}{1400} & 0 & 0 \\ -\frac{1}{1400} & \frac{11}{6300} & 0 & 0 \\ 0 & 0 & \frac{1}{700} & \frac{1}{1400} \\ 0 & 0 & \frac{1}{1400} & \frac{11}{6300} \end{bmatrix},$$

$$[H_3] \triangleq \frac{1}{4}\begin{bmatrix} 0 & 0 & 0 & -2 \\ 0 & 0 & -2 & -1 \\ 0 & -2 & 0 & 0 \\ -2 & -1 & 0 & 0 \end{bmatrix}$$

$$[H_5] \triangleq \frac{1}{60}\begin{bmatrix} 0 & 0 & 0 & 1 \\ 0 & 0 & 1 & 0 \\ 0 & 1 & 0 & 0 \\ 1 & 0 & 0 & 0 \end{bmatrix}, [H_6] \triangleq \frac{1}{20}\begin{bmatrix} 4 & -2 & 0 & 0 \\ -2 & 1 & 0 & 0 \\ 0 & 0 & 4 & 2 \\ 0 & 0 & 2 & 1 \end{bmatrix}$$

$$[H_7] \triangleq \begin{bmatrix} 0 & 0 & 0 & 0 \\ 0 & 0 & 0 & 1 \\ 0 & 0 & 0 & 0 \\ 0 & 0 & 0 & 0 \end{bmatrix}$$

All nonlinear effects that are significant when the translational and angular displacement range of the beam end is limited to 0.1$L$ and 0.1 radians, respectively, are captured in Eqs. -(15). On setting $\beta$ and $\gamma$ to zero, Eq.(12) -

(15) reduce to the known results of a non-tilted spatial beam [3]. Equation (12), which is the transverse load-displacement relation, expresses bending loads $\{\boldsymbol{f}_{y1} \quad \boldsymbol{m}_{z1} \quad \boldsymbol{f}_{z1} \quad \boldsymbol{m}_{y1}\}$ as a product of bending stiffness values and bending displacement.

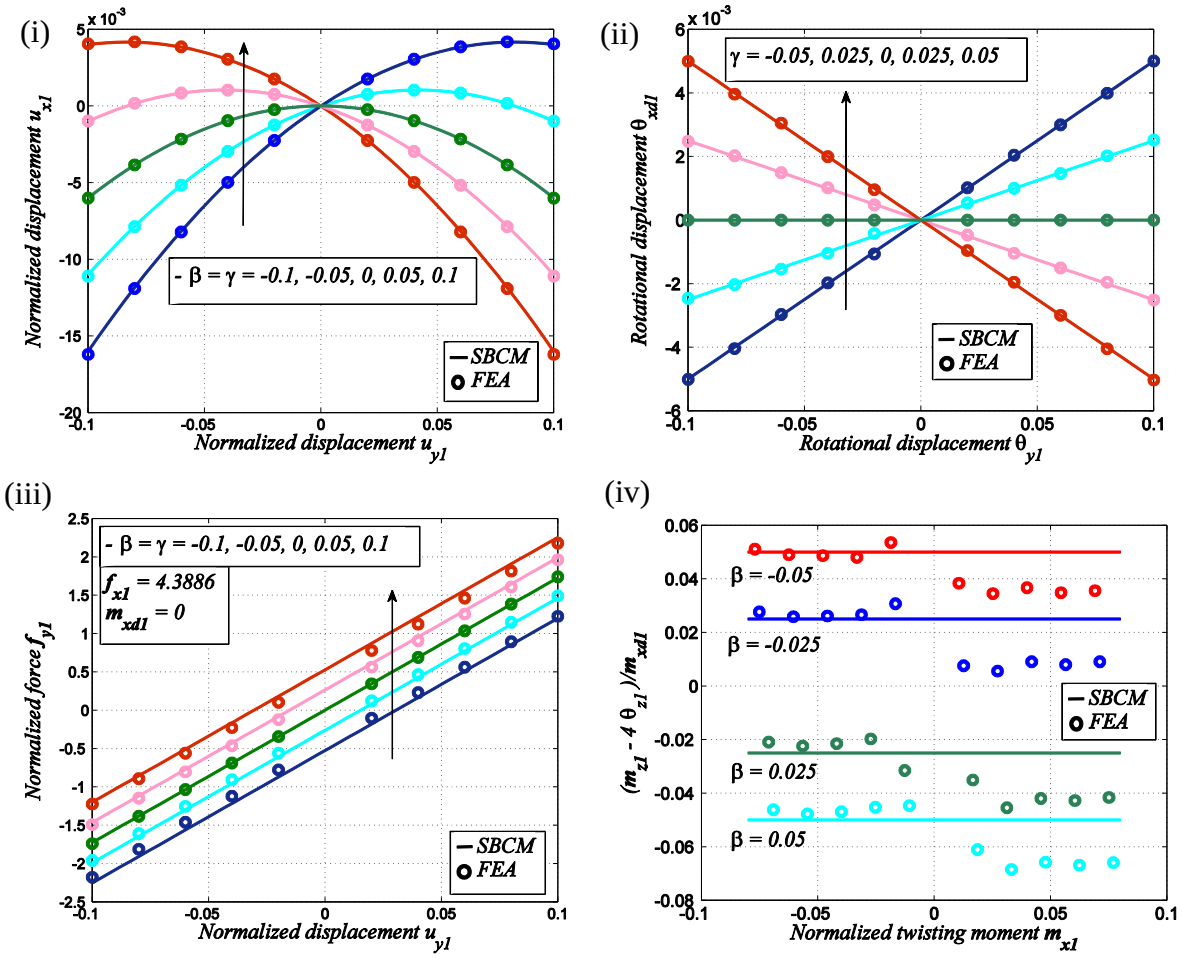


*Figure 4:(i) Normalized force $\boldsymbol{f}_{y1}$ vs normalized displacement $u_{y1}$ for varying tilt angle $\beta$ and $\gamma$ (ii) Normalized $(\boldsymbol{m}_{z1}-4\theta_{z1})/\boldsymbol{m}_{xd1}$ vs normalized moment $\boldsymbol{m}_{x1}$ at $\theta_{y1}=0$ and $\theta_{z1}=0.02$ radians for varying tilt angle $\beta$ (iii) Normalized displacement $u_{x1}$ vs normalized displacement $u_{y1}$ for varying $\beta$ and $\gamma$ (iv) Rotational displacement $\theta_{xd1}$ vs Rotational displacement $\theta_{y1}$ for varying $\gamma$*

The first term in Eq. (12), $[H_1]\{u_{y1} \quad u'_{y1} \quad u_{z1} \quad -u'_{z1}\}^T$, captures the linear bending stiffness values of $d\boldsymbol{f}_{y1}/du_{y1}$, $d\boldsymbol{f}_{z1}/du_{z1}$, $d\boldsymbol{m}_{y1}/du'_{z1}$ and $d\boldsymbol{m}_{z1}/du'_{y1}$ and can be easily shown to be in agreement with the linear load-

displacement curves for cantilever beams [17]. The first and second powers of $\boldsymbol{f_{x1}}$ and $\boldsymbol{m_{xd1}}$ in the bending stiffness values capture the variation in bending stiffnesses due to axial loads. In particular, the stiffness terms with single power of $\boldsymbol{f_{x1}}$ and $\boldsymbol{m_{xd1}}$ are a result of the geometric arc length conservation and are called load or geometric stiffening terms [17]. The terms that are quadratic in $\boldsymbol{f_{x1}}$ and $\boldsymbol{m_{xd1}}$ are relatively less significant than the load stiffening terms but are retained to maintain truncation consistency with Eqs. (13) and (14). Due to the initial beam tilt, the load displacement curves shift while maintaining the stiffness values. This curve shift is more significant for the transverse force ($\boldsymbol{f_{y1}}$ or $\boldsymbol{f_{z1}}$) vs. transverse displacement ($u_{y1}$ or $u_{z1}$) as shown in Figure 4(i). For the transverse moment vs. transverse rotation curve, the shifts due to tilt angles $\beta$ and $\gamma$ (i.e. $\boldsymbol{m_{xd1}}\, u'_{z1}$ in $\boldsymbol{m_{y1}}$ vs. $u'_{z1}$, and $-\boldsymbol{m_{xd1}}\, u'_{y1}$ in $\boldsymbol{m_{z1}}$ vs. $u'_{y1}$ ) are much smaller due to the limited range of $u'_{z1}$ and $u'_{y1}$. However, this shift becomes crucial for an accurate determination of bending moments, $\boldsymbol{m_{y1}}$ and $\boldsymbol{m_{z1}}$, at small bending angles. For a small angle, $u'_{y1}$ = 0.02 rad, Figure 4(ii) plots this curve shift divided by $\boldsymbol{m_{xd1}}$ for varying $\boldsymbol{m_{x1}}$. Noticeable fluctuations are seen in the FEA validation results, indicating that this term is of the order of other second approximations made during model derivation.

Equation(13), which quantifies the axial displacement $u_{x1}$, is the constraint equation because of the inherent high stiffness in the axial stretching direction with respect to the bending direction. The first two terms in Eq. represent the elastic stretching of the beam due to $\boldsymbol{f_{x1}}$ and $\boldsymbol{m_{xd1}}$. The stretching due to $\boldsymbol{m_{xd1}}$ is the well-known trapeze effect, which occurs due to the additional axial stresses developed during torsion by unequal contraction of axial fibers parallel to but at different distance from the centroidal axis of the beam. The third term in Eq. (13), that is dependent only on transverse displacements due to bending represents the shortening of the projection of the beam on the X-axis due to the geometric arc length conservation. The fourth and the fifth terms represent additional kinematic relation between the bending displacements and axial displacement $u_{x1}$. This kinematic behavior is shown in Figure 4(iii). Essentially due to the tilt, the parabola in the $u_{x1}$ vs. $u_{y1}$ plot gets shift vertically as well as horizontally. The fourth term in Eq. (13), which is dependent on both displacements and loads, $\boldsymbol{f_{x1}}$ and $\boldsymbol{m_{xd1}}$, represents a variation in the amount of shortening of the projection of the beam on the X-axis as $\boldsymbol{f_{x1}}$ and $\boldsymbol{m_{xd1}}$ change the shape of a bent beam by producing additional bending moments. From a different point of view, this term quantifies the softening of the X direction stiffness of a deformed (i.e. bent) beam with respect to a straight beam. Since this term is non-zero only in the presence of both loads and displacements, it is an elastokinematic effect. It should be noted that tilt angles $\beta$ and $\gamma$ have no significant impact on the axial stiffness.

Equation (14) parametrically quantifies the dependence of the twist $\theta_{xd1}$ on the axial and torsional loads, $\boldsymbol{f}_{x1}$ and $\boldsymbol{m}_{xd1}$, and transverse bending displacements. Similar to Eq.(13), elastic, kinematic/geometric and elastokinematic terms are present. The only difference is that the trapeze effect can only vary stiffness rather than produce an independent twist displacement as in the case of Eq. (13). Tilt angle $\gamma$ gives rise to an additional kinematic dependence of twist $\theta_{xd1}$ on bending displacements. This relation is verified using FEA in Figure 4(iv). It is interesting that tilt angle $\beta$ does not affect twist $\theta_{xd1}$, but not surprising because the sequential definition of the Euler angles introduces a lack of symmetry between beta and gamma in the formulation. Because of the mathematical similarity with Eq. (13), Eq.(14) is also referred to as a constraint equation in spite of a relatively low stiffness in the twisting direction.

Equation (15) represents the total strain energy stored in the beam in the presence of end-displacements, $u_{x1}$ and $\theta_{xd1}$. The first, second, and third terms are really functions of displacements, but are written in terms of axial and torsional loads, $\boldsymbol{f}_{x1}$ and $\boldsymbol{m}_{xd1}$, for convenience and compactness of representation. Terms associated with $[H_2]$, $[H_3]$ and $[H_7]$ correspond to purely kinematic effect, and hence have no contribution to the strain energy. However, the strain energy due to the elastokinematic effects is captured via the terms with quadratic powers of $\boldsymbol{f}_{x1}$ and $\boldsymbol{m}_{xd1}$. Since $\beta$ and $\gamma$ shows up in load-stiffening effect in bending and kinematic stretching and twisting, all of which are non-elastic effects, these angles have no effect on the strain energy.

Therefore, with Eqs.(12) -(15), even if the beam is tilted, the SBCM can still be expressed in the global co-ordinate frame X-Y-Z rather than tilted co-ordinate frame $X_T$-$Y_T$-$Z_T$. It should be noted that if the tilt in the spatial beam flexure also has a rotational misalignment of α about the X axis, the SBCM can be easily modified to be expressed in the global co-ordinate frame by replacing the bending displacements $u_{y1}$, $u_{z1}$, $u'_{y1}$ and $u'_{z1}$ by $u_{y1}\cos(\alpha)-u_{z1}\sin(\alpha)$, $u_{z1}\cos(\alpha)+u_{y1}\sin(\alpha)$, $u'_{y1}\cos(\alpha)-u'_{z1}\sin(\alpha)$ and $u'_{z1}\cos(\alpha)+u'_{y1}\sin(\alpha)$ and the bending loads $\boldsymbol{f}_{y1}$, $\boldsymbol{f}_{z1}$, $\boldsymbol{m}_{y1}$ and $\boldsymbol{m}_{z1}$ by $\boldsymbol{f}_{y1}\cos(\alpha)-\boldsymbol{f}_{z1}\sin(\alpha)$, $\boldsymbol{f}_{z1}\cos(\alpha)+\boldsymbol{f}_{y1}\sin(\alpha)$, $\boldsymbol{m}_{y1}\cos(\alpha)-\boldsymbol{m}_{y1}\sin(\alpha)$ and $\boldsymbol{m}_{z1}\cos(\alpha)+\boldsymbol{m}_{y1}\sin(\alpha)$.

The primary change in the SBCM due to the addition X rotation α is that the beam characteristics $[H]$ matrices for the global co-ordinate frame in this case needs to be calculated from the beam characteristics $[H]$ matrices in Eqs. (12) -(15) as

$$= [R]\left[H_i\right][R]^T \quad \text{for } i = 1,..,7$$

$$\text{where} \quad [R] \triangleq \begin{bmatrix} c(\alpha) & 0 & s(\alpha) & 0 \\ 0 & c(\alpha) & 0 & -s(\alpha) \\ -s(\alpha) & 0 & c(\alpha) & 0 \\ 0 & s(\alpha) & 0 & c(\alpha) \end{bmatrix} \tag{16}$$

$$c(\alpha) \triangleq \cos(\alpha), \quad s(\alpha) \triangleq \sin(\alpha)$$

## 3. FUNDAMENTAL RELATIONS BETWEEN BEAM CHARACTERISTIC COEFFICIENTS

We next proceed to generalize the SBCM further by showing that for the structure of SBCM is invariant for slender beams[2] with variable cross-section and only the [*H*] matrices change in its numerical value. The main utility of such a generalized model is that a closed-form model of any flexure mechanism that uses flexure elements with varying cross-sections rather than only simple prismatic beams can be derived without any additional mathematical complexity.

Let the area moment of inertias of a slender beam with a bisymmetrical but otherwise arbitrary cross-section that varies along the length be represented by $I_{YY}(X) = I_{ZZ}(X) = I_0\xi(X)$ where $I_0$ is the cross-section at X=0. Similarly, let the area and the torsion constant be $A_0 f_1\left(\xi(X)\right)$ and $J_0 f_2\left(\xi(X)\right)$ respectively. Here, it is assumed that $\xi(0) = 1$ thus implying that $A_0$ and $J_0$ are the area and torsion constant at X=0 while $f_1$ and $f_2$ are functions of $\xi(X)$. The normalization scheme remains the same as Eq.(8), with the exception that $I_0$ is now used in place of $I$. Using the same modeling assumptions and following a PVW procedure analogous to the one outlined in Sec. 2, one may derive the following normalized governing equations and natural boundary conditions for this case as

$$\begin{aligned} &\left\{\xi(x)u_y''\right\}'' - \boldsymbol{f}_{x1}u_y'' + \boldsymbol{m}_{xd1}u_z''' = 0; \\ &\left\{\xi(x)u_z''\right\}'' - \boldsymbol{f}_{x1}u_z'' - \boldsymbol{m}_{xd1}u_y''' = 0 \end{aligned} \tag{17}$$

$$\begin{aligned} &u_x' + \frac{1}{2}u_y'^2 + \frac{1}{2}u_z'^2 = \frac{\boldsymbol{f}_{x1}}{\bar{k}_x} - \frac{\boldsymbol{m}_{xd1}^2}{\bar{k}_x\bar{k}_\theta^2}; \\ &\theta_{xd}' - u_z''\,u_y' \approx \frac{\boldsymbol{m}_{xd1}}{\bar{k}_\theta} - \frac{2\boldsymbol{m}_{xd1}\boldsymbol{f}_{x1}}{\bar{k}_x\bar{k}_\theta^2} \end{aligned} \tag{18}$$

[2] A slender beam is defined as a beam, the thickness and width of which are at least 1/20th of its length.

$$
\begin{aligned}
\boldsymbol{f}_{y1} &= \boldsymbol{f}_{x1}u'_{y1} - \xi(x)u'''_{y1} - \boldsymbol{m}_{xd1}u''_{z1};\\
\boldsymbol{f}_{z1} &= \boldsymbol{f}_{x1}u'_{z1} - \xi(x)u'''_{z1} + \boldsymbol{m}_{xd1}u''_{y1}\\
\boldsymbol{m}_{y1} &= -\xi(x)u''_{z1} + \boldsymbol{m}_{xd1}u'_{y1};\\
\boldsymbol{m}_{z1} &= \xi(x)u''_{y1} + \boldsymbol{m}_{xd1}u'_{z1}
\end{aligned}
\tag{19}
$$

Here $\bar{k}_x$ and $\bar{k}_\theta$ are the linear elastic stretching and twisting stiffness values associated with the beam with varying cross-section.

Given the arbitrary choice of $\xi(X)$, a closed-form solution to this ordinary differential equation with variable coefficients (Eq.(17)) is no longer trivial. Nevertheless, the bending direction governing equations in Eq.(17) and associated boundary conditions in Eq.(19) remain linear in the transverse loads $\left(\boldsymbol{f}_{y1}, \boldsymbol{f}_{z1}, \boldsymbol{m}_{y1}, \text{and } \boldsymbol{m}_{z1}\right)$ and transverse displacements ($u_{y1}$ and $u_{z1}$ and its derivatives). This implies that the resulting normalized relation between the transverse end-loads and end displacement also has to be linear, of the form

$$
\begin{Bmatrix} \boldsymbol{f}_{y1} \\ \boldsymbol{m}_{z1} \\ \boldsymbol{f}_{z1} \\ \boldsymbol{m}_{y1} \end{Bmatrix} = \left[k\left(\boldsymbol{f}_{x1}; \boldsymbol{m}_{xd1}; \xi(x)\right)\right] \begin{Bmatrix} u_{y1} \\ u'_{y1} \\ u_{z1} \\ -u'_{z1} \end{Bmatrix}
$$

where $[k] \triangleq \begin{bmatrix} k_{11} & k_{12} & k_{13} & k_{14} \\ k_{21} & k_{22} & k_{23} & k_{24} \\ k_{31} & k_{32} & k_{33} & k_{34} \\ k_{41} & k_{42} & k_{43} & k_{44} \end{bmatrix}$

The effective stiffness terms ($k$'s) will now be some functions of the axial loads $\boldsymbol{f}_{x1}$ and $\boldsymbol{m}_{xd1}$, dictated by the beam shape $\xi(X)$ and might be difficult or impossible to determine in closed form. Nevertheless, these functions may certainly be expanded as a generic infinite series in $\boldsymbol{f}_{x1}$ and $\boldsymbol{m}_{xd1}$,

$$
\begin{Bmatrix} \boldsymbol{f}_{y1} \\ \boldsymbol{m}_{z1} \\ \boldsymbol{f}_{z1} \\ \boldsymbol{m}_{y1} \end{Bmatrix} = \sum_{n=0}^{\infty}\sum_{i=0}^{n} \boldsymbol{f}_{x1}^{n-i}\boldsymbol{m}_{xd1}^{i}\left[k^{(n-i,i)}\right] \begin{Bmatrix} u_{y1} \\ u'_{y1} \\ u_{z1} \\ -u'_{z1} \end{Bmatrix}
\tag{20}
$$

Similarly, it may be shown that irrespective of the beam shape, the solution to the constraint equations (18) will be quadratic in bending displacements $u_{y1}$, $u_{z1}$, $u'_{y1}$ and $u'_{z1}$ and therefore may be expanded as

$$u_{x1} = \frac{\boldsymbol{f_{x1}}}{\bar{k}_x} - \frac{\boldsymbol{m_{xd1}^2}}{\bar{k}_\theta^2 \bar{k}_x} + \sum_{n=0}^{\infty}\sum_{i=0}^{n} \boldsymbol{f_{x1}}^{n-i} \boldsymbol{m_{xd1}}^{i} \begin{Bmatrix} u_{y1} \\ u'_{y1} \\ u_{z1} \\ -u'_{z1} \end{Bmatrix}^T \left[ g^{(n-i,i)} \right] \begin{Bmatrix} u_{y1} \\ u'_{y1} \\ u_{z1} \\ -u'_{z1} \end{Bmatrix} \tag{21}$$

$$\theta_{xd1} = \frac{\boldsymbol{m_{xd1}}}{\bar{k}_\theta} - \frac{2\boldsymbol{m_{xd1}}\boldsymbol{f_{x1}}}{\bar{k}_x \bar{k}_\theta^2} + \sum_{n=0}^{\infty}\sum_{i=0}^{n} \boldsymbol{f_{x1}}^{n-i} \boldsymbol{m_{xd1}}^{i} \begin{Bmatrix} u_{y1} \\ u'_{y1} \\ u_{z1} \\ -u'_{z1} \end{Bmatrix}^T \left[ e^{(n-i,i)} \right] \begin{Bmatrix} u_{y1} \\ u'_{y1} \\ u_{z1} \\ -u'_{z1} \end{Bmatrix} \tag{22}$$

Here $[g^{(n-i,i)}]$ and $[e^{(n-i,i)}]$ are 4×4 matrices similar to $[k^{(n-i,i)}]$.

Along the same lines, the strain energy for a variable cross-section beam may be shown to be quadratic in the transverse displacements $u_{y1}$, $u_{z1}$, $\theta_{y1}$ and $\theta_{z1}$, and some unknown function of the loads $\boldsymbol{f_{x1}}$ and $\boldsymbol{m_{xd1}}$. This expression may be expanded as follows:

$$v = \frac{\boldsymbol{m_{xd1}^2}}{2\bar{k}_\theta} + \frac{\boldsymbol{f_{x1}^2}}{2\bar{k}_x} - \frac{2\boldsymbol{m_{xd1}^2}\boldsymbol{f_{x1}}}{\bar{k}_x \bar{k}_\theta^2} + \frac{1}{2}\sum_{n=0}^{\infty}\sum_{i=0}^{n} \boldsymbol{f_{x1}}^{n-i} \boldsymbol{m_{xd1}}^{i} \begin{Bmatrix} u_{y1} \\ u'_{y1} \\ u_{z1} \\ -u'_{z1} \end{Bmatrix}^T \left[ v^{(n-i,i)} \right] \begin{Bmatrix} u_{y1} \\ u'_{y1} \\ u_{z1} \\ -u'_{z1} \end{Bmatrix} \tag{23}$$

The 4×4 matrices in equations (20) - (23), $[k^{(n-i,i)}]$, $[g^{(n-i,i)}]$, $[e^{(n-i,i)}]$ and $[v^{(n-i,i)}]$, are constants dependent only on the shape of the beam, i.e. $\xi(X)$, but independent of end-loads and end-displacements. Here onwards, these coefficients will be referred to as *beam characteristic coefficients*.

The first three terms of Eq.(23) represent the energy due to elastic stretching and elastic twisting, and are related to first two terms of Eqs. (21) and (22). Although these energy terms should ideally be represented using displacement variables, in this case these are expressed in terms of loads for simplicity and compactness of representation. The fourth term in Eq. (23) represents the energy due to bending. Ideally this energy term should consist of only bending displacements $u_{y1}$, $u_{z1}$, $\theta_{y1}$ and $\theta_{z1}$. However, due to geometric nonlinearity, the actual beam shape is dependent on the axial loads $\boldsymbol{f_{x1}}$ and $\boldsymbol{m_{xd1}}$. As a result, $\boldsymbol{f_{x1}}$ and $\boldsymbol{m_{xd1}}$ appear in strain energy due to bending, as parameters in the same manner as the beam shape parameter $\xi(X)$ and the beam characteristic coefficients.

The PVW for the normalized displacement co-ordinates of $\delta u_{x1}$, $\delta u_{y1}$, $\delta u_{z1}$, $\delta\theta_{xd1}$, $\delta u'_{y1}$ and $\delta u'_{z1}$ and normalized loads $\boldsymbol{f_{x1}}$, $\boldsymbol{f_{y1}}$, $\boldsymbol{f_{z1}}$, $\boldsymbol{m_{xd1}}$, $\boldsymbol{m_{y1}}$ and $\boldsymbol{m_{z1}}$ is given below [3].

$$\begin{aligned}\delta v = {} & \boldsymbol{f_{x1}}\delta u_{x1} + \boldsymbol{f_{y1}}\delta u_{y1} + \boldsymbol{f_{z1}}\delta u_{z1} + \boldsymbol{m_{xd1}}\delta\theta_{xd1} \\ & -\boldsymbol{m_{y1}}\delta u'_{z1} + \left(\boldsymbol{m_{z1}} - \boldsymbol{m_{xd1}}u'_{z1}\right)\delta u'_{y1}\end{aligned} \tag{24}$$

The variation of the strain energy is taken, keeping in mind that loads are kept constant while virtual displacements are applied. Therefore, the loads $\boldsymbol{f_{x1}}$ and $\boldsymbol{m_{xd1}}$ in the strain energy due to bending do not produce $\delta\boldsymbol{f_{x1}}$ and $\delta\boldsymbol{m_{xd1}}$. By applying PVW, the portion of the energy due to elastic stretching, twisting and trapeze effect simply leads to the elastic stretching and twisting components of $u_{x1}$ and $\theta_{xd1}$. Additionally, PVW also relates [$k$] matrices of the transverse load-displacement relation to the [$g$], [$e$] and [$v$] matrices of the constraint relations and strain energy expression as follows:

$$\begin{aligned}&\left[k^{(0,0)}\right] = \left[v^{(0,0)}\right] \\ &\left[k^{(a,0)}\right] = \left[v^{(a,0)}\right] - 2\left[g^{(a-1,0)}\right] \qquad \forall\ a = 1,2,3,.... \\ &\left[k^{(0,1)}\right] + \left[H_7\right] = \left[v^{(0,1)}\right] - 2\left[e^{(0,0)}\right]\end{aligned} \tag{25}$$

$$\begin{aligned}&\left[k^{(0,b)}\right] = \left[v^{(0,b)}\right] - 2\left[e^{(0,b-1)}\right] \qquad \forall\ b = 2,3,.... \\ &\left[k^{(a,b)}\right] = \left[v^{(a,b)}\right] - 2\left[g^{(a-1,b)}\right] - 2\left[e^{(a,b-1)}\right],\ \forall a,b = 1,2,3,....\end{aligned}$$

The above relations may be readily verified for the case of a simple spatial beam using known results [3]; however, it should be noted that these are valid for any general beam shape, as proven above.

Next, using the conservation of energy, yet another fundamental relation between the beam characteristic coefficients can be found. Since a given set of end-loads $\boldsymbol{f_{x1}}$, $\boldsymbol{f_{y1}}$, $\boldsymbol{f_{z1}}$, $\boldsymbol{m_{xd1}}$, $\boldsymbol{m_{y1}}$ and $\boldsymbol{m_{z1}}$ produces a unique set of end-displacements $u_{x1}$, $u_{y1}$, $u_{z1}$, $\theta_{xd1}$, $u'_{y1}$ and $u'_{z1}$, the resulting strain energy stored in the deformed beam remains the same irrespective of the order in which the loading is carried out. Therefore, we consider a case where the loading is performed in three steps: (i) Some end-loads $\bar{\boldsymbol{f}}_{y1}$, $\bar{\boldsymbol{f}}_{z1}$, $\bar{\boldsymbol{m}}_{y1}$ and $\bar{\boldsymbol{m}}_{z1}$ are applied to produce the final bending end-displacements $u_{y1}, u_{z1}, u'_{z1}$, and $u'_{y1}$ and some end-displacements $\bar{u}_{x1}$ and $\bar{\theta}_{xd1}$ along X. (ii) While holding the end-displacements $u_{y1}$, $u_{z1}$, $u'_{z1}$, and $u'_{y1}$ fixed, the end-load $\boldsymbol{f_{x1}}$ is applied to change the axial displacement from $\bar{u}_{x1}$ to $\bar{\bar{u}}_{x1}$. Due to $\boldsymbol{f_{x1}}$, $\bar{\theta}_{xd1}$ changes to $\bar{\bar{\theta}}_{xd1}$. The transverse end-loads change to $\bar{\bar{\boldsymbol{f}}}_{y1}$, $\bar{\bar{\boldsymbol{f}}}_{z1}$, $\bar{\bar{\boldsymbol{m}}}_{y1}$ and $\bar{\bar{\boldsymbol{m}}}_{z1}$ to maintain the transverse displacements. (iii) While holding the end-displacements $u_{y1}$, $u_{z1}$, $u'_{z1}$, and $u'_{y1}$ and end-load $\boldsymbol{f_{x1}}$ fixed, end-load

$\boldsymbol{m_{xd1}}$ is applied to change the axial displacement from $\bar{\bar{\theta}}_{xd1}$ to $\theta_{xd1}$. Due to end-load $\boldsymbol{m_{xd1}}$, end displacement $\bar{\bar{u}}_{x1}$ changes to $u_{x1}$ as well. Also, with $\boldsymbol{f_{x1}}$ and $\boldsymbol{m_{xd1}}$ applied end-loads $\bar{\bar{\boldsymbol{f}}}_{\boldsymbol{y1}}$, $\bar{\bar{\boldsymbol{f}}}_{\boldsymbol{z1}}$, $\bar{\bar{\boldsymbol{m}}}_{\boldsymbol{y1}}$ and $\bar{\bar{\boldsymbol{m}}}_{\boldsymbol{z1}}$ will change to $\boldsymbol{f}_{\boldsymbol{y1}}$, $\boldsymbol{f}_{\boldsymbol{z1}}$, $\boldsymbol{m}_{\boldsymbol{y1}}$ and $\boldsymbol{m}_{\boldsymbol{z1}}$ in order to maintain $u_{y1}$, $u_{z1}$, $u'_{z1}$, and $u'_{y1}$.

The sum of energy added to the beam in these three steps should be equal to the final strain energy given by Eq. (23). Energy stored in step 1 is simply obtained by setting $\boldsymbol{f_{x1}}$ and $\boldsymbol{m_{xd1}}$=0 in Eq.(23).

$$v_1 = \frac{1}{2}\begin{Bmatrix} u_{y1} & u'_{y1} & u_{z1} & -u'_{z1} \end{Bmatrix}\begin{bmatrix} v^{(0,0)} \end{bmatrix}\begin{Bmatrix} u_{y1} & u'_{y1} & u_{z1} & -u'_{z1} \end{Bmatrix}^T \tag{26}$$

The axial displacement and rotation at the end of step 1 are given by

$$\bar{u}_{x1} = \begin{Bmatrix} u_{y1} & u'_{y1} & u_{z1} & -u'_{z1} \end{Bmatrix}\begin{bmatrix} g^{(0,0)} \end{bmatrix}\begin{Bmatrix} u_{y1} & u'_{y1} & u_{z1} & -u'_{z1} \end{Bmatrix}^T \tag{27}$$

$$\bar{\theta}_{xd1} = \begin{Bmatrix} u_{y1} & u'_{y1} & u_{z1} & -u'_{z1} \end{Bmatrix}\begin{bmatrix} e^{(0,0)} \end{bmatrix}\begin{Bmatrix} u_{y1} & u'_{y1} & u_{z1} & -u'_{z1} \end{Bmatrix}^T \tag{28}$$

Next, assuming a conservative system, the energy added to the beam in step 2 may simply be determined by calculating the work done on the system when force $\boldsymbol{f_{x1}}$ causes the beam end to move from $\bar{u}_{x1}$ to $\bar{\bar{u}}_{x1}$ in the axial direction. End-displacement $\bar{\bar{u}}_{x1}$ can be easily calculated by setting $\boldsymbol{m_{xd1}}$=0 in Eq.(21).

$$\begin{aligned} \bar{\bar{u}}_{x1} &= \frac{\boldsymbol{f_{x1}}}{\bar{k}_x} \\ &+ \sum_{n=0}^{\infty} \boldsymbol{f}_{\boldsymbol{x1}}^{\,n} \begin{Bmatrix} u_{y1} & u'_{y1} & u_{z1} & -u'_{z1} \end{Bmatrix}\begin{bmatrix} g^{(n,0)} \end{bmatrix}\begin{Bmatrix} u_{y1} & u'_{y1} & u_{z1} & -u'_{z1} \end{Bmatrix}^T \end{aligned} \tag{29}$$

An integral needs to be carried out since the relation between $\boldsymbol{f_{x1}}$ and $u_{x1}$ is nonlinear. However, since inverting Eq.(29), which provides displacement in terms of force, is not trivial, determining the work done in this fashion is difficult if not impossible. Therefore, instead we choose to determine the complementary energy, which is readily derived using Eq.(27) and(29):

$$v_2^*\left(\boldsymbol{f_{x1}}\right) = \int_0^{f_{x1}} \left(\bar{\bar{u}}_{x1} - \bar{u}_{x1}\right).d\boldsymbol{f_{x1}} \tag{30}$$

This result is then used to calculate the strain energy stored in the beam during step 2 as follows:

$$v_2\left(\boldsymbol{f_{x1}}\right)=\left(\bar{\bar{u}}_{x1}-\bar{u}_{x1}\right).\boldsymbol{f_{x1}}-v_2^*\left(\boldsymbol{f_{x1}}\right)$$
$$=\frac{\boldsymbol{f_{x1}^2}}{2\bar{\bar{k}}_x}+\sum_{n=0}^{\infty}\frac{(n-1)\,\boldsymbol{f_{x1}^n}}{n}\begin{Bmatrix}u_{y1}\\u'_{y1}\\u_{z1}\\-u'_{z1}\end{Bmatrix}^T\left[g^{(n-1,0)}\right]\begin{Bmatrix}u_{y1}\\u'_{y1}\\u_{z1}\\-u'_{z1}\end{Bmatrix}$$

The twisting angle $\bar{\bar{\theta}}_{xd1}$ can be calculated by setting $\boldsymbol{m_{xd1}}$=0 in Eq.(22).

$$\bar{\bar{\theta}}_{xd1}=\sum_{n=0}^{\infty}\boldsymbol{f_{x1}^n}\begin{Bmatrix}u_{y1}\\u'_{y1}\\u_{z1}\\-u'_{z1}\end{Bmatrix}^T\left[e^{(n,0)}\right]\begin{Bmatrix}u_{y1}\\u'_{y1}\\u_{z1}\\-u'_{z1}\end{Bmatrix} \tag{31}$$

Next, the energy added to the beam in step 3 may simply be determined by calculating the sum of work done on the system when moment $\boldsymbol{m_{xd1}}$ causes the beam end to twist from $\bar{\bar{\theta}}_{xd1}$ to $\theta_{xd1}$, denoted as $v_{31}\left(\boldsymbol{m_{xd1}}\right)$, and work done when the beam end moves $\bar{\bar{u}}_{x1}$ to $u_{x1}$ against constant force $\boldsymbol{f_{x1}}$, denoted as $v_{32}\left(\boldsymbol{m_{xd1}}\right)$. The first term, $v_{31}\left(\boldsymbol{m_{xd1}}\right)$, is calculated in the same way as done in step 2.

$$v_{31}\left(\boldsymbol{m_{xd1}}\right)=\left(\theta_{xd1}-\bar{\bar{\theta}}_{xd1}\right).\boldsymbol{m_{xd1}}-v_3^*\left(\boldsymbol{m_{xd1}}\right)=\frac{\boldsymbol{m_{xd1}^2}}{2\bar{\bar{k}}_\theta}-\frac{\boldsymbol{m_{xd1}^2}\,\boldsymbol{f_{x1}}}{\bar{\bar{k}}_x\bar{\bar{k}}_\theta^2}$$
$$+\sum_{n=0}^{\infty}\sum_{i=1}^{n}\frac{i\boldsymbol{f_{x1}^{n-i}}\boldsymbol{m_{xd1}^{i+1}}}{i+1}\begin{Bmatrix}u_{y1}\\u'_{y1}\\u_{z1}\\-u'_{z1}\end{Bmatrix}^T\left[e^{(n-i,i)}\right]\begin{Bmatrix}u_{y1}\\u'_{y1}\\u_{z1}\\-u'_{z1}\end{Bmatrix} \tag{32}$$

The second term, $v_{32}\left(\boldsymbol{m_{xd1}}\right)$, in step 3 is

$$v_{32}\left(\boldsymbol{f_{x1}}\right)=\left(u_{x1}-\bar{\bar{u}}_{xd1}\right).\boldsymbol{f_{x1}}$$
$$=-\frac{\boldsymbol{m_{xd1}^2}\,\boldsymbol{f_{x1}}}{\bar{\bar{k}}_\theta^2\bar{\bar{k}}_x}+\sum_{n=0}^{\infty}\sum_{i=1}^{n}\boldsymbol{f_{x1}^{n-i+1}}\boldsymbol{m_{xd1}^i}\begin{Bmatrix}u_{y1}\\u'_{y1}\\u_{z1}\\-u'_{z1}\end{Bmatrix}^T\left[g^{(n-i,i)}\right]\begin{Bmatrix}u_{y1}\\u'_{y1}\\u_{z1}\\-u'_{z1}\end{Bmatrix} \tag{33}$$

Therefore the total strain energy in the beam due to the application of $\boldsymbol{f_{x1}}$, $\boldsymbol{f_{y1}}$, $\boldsymbol{f_{z1}}$, $\boldsymbol{m_{x1}}$, $\boldsymbol{m_{y1}}$ and $\boldsymbol{m_{z1}}$ resulting in end-displacements, $u_{x1}$, $u_{y1}$, $u_{z1}$, $\theta_{xd1}$, $u'_{y1}$ and $u'_{z1}$, calculated using step (i), (ii) and (iii) is given by

$$v = \frac{\boldsymbol{f}_{x1}^2}{2\bar{k}_x} + \frac{\boldsymbol{m}_{xd1}^2}{2\bar{k}_\theta} - \frac{2\boldsymbol{m}_{xd1}^2 \boldsymbol{f}_{x1}}{\bar{k}_x \bar{k}_\theta^2}$$
$$+\frac{1}{2}\begin{Bmatrix} u_{y1} \\ u'_{y1} \\ u_{z1} \\ -u'_{z1} \end{Bmatrix}^T \begin{pmatrix} \left[ v^{(0,0)} \right] \\ +2\sum_{n=1}^{\infty} \frac{(n-1)\,\boldsymbol{f}_{x1}^n}{n} \left[ g^{(n-1,0)} \right] \\ +2\sum_{n=1}^{\infty}\sum_{i=1}^{n} \frac{i\boldsymbol{f}_{x1}^{n-i}\boldsymbol{m}_{xd1}^{i+1}}{i+1} \left[ e^{(n-i,i)} \right] \\ +2\sum_{n=1}^{\infty}\sum_{i=1}^{n} \boldsymbol{f}_{x1}^{n-i+1}\boldsymbol{m}_{xd1}^{i} \left[ g^{(n-i,i)} \right] \end{pmatrix} \begin{Bmatrix} u_{y1} \\ u'_{y1} \\ u_{z1} \\ -u'_{z1} \end{Bmatrix} \tag{34}$$

Comparing Eqs.(23) and (34), we obtain the following relations between the beam characteristic coefficients.

$$\begin{aligned} &\frac{1}{2}\left[ v^{(a,0)} \right] = \frac{a-1}{a}\left[ g^{(a-1,0)} \right] \qquad \forall \;\; a = 1,2,3,.. \\ &\frac{1}{2}\left[ v^{(0,b)} \right] = \frac{b-1}{b}\left[ e^{(0,b-1)} \right] \qquad \forall \;\; \mathrm{b} = 1,2,3,.. \\ &\frac{1}{2}\left[ v^{(a,b)} \right] = \left[ g^{(a-1,b)} \right] + \frac{b-1}{b}\left[ e^{(a,b-1)} \right] \qquad \forall \;\; a,b = 1,2,3,.. \end{aligned} \tag{35}$$

Alternatively, the conservation of energy could have also been applied while interchanging steps (ii) and (iii). In that case the relations between the beam characteristic coefficients would have been as follows:

$$\begin{aligned} &\frac{1}{2}\left[ v^{(a,0)} \right] = \frac{a-1}{a}\left[ g^{(a-1,0)} \right] \qquad \forall \;\; a = 1,2,3,.. \\ &\frac{1}{2}\left[ v^{(0,b)} \right] = \frac{b-1}{b}\left[ e^{(0,b-1)} \right] \qquad \forall \;\; \mathrm{b} = 1,2,3,.. \\ &\frac{1}{2}\left[ v^{(a,b)} \right] = \left[ e^{(a,b-1)} \right] + \frac{a-1}{a}\left[ g^{(a-1,b)} \right] \qquad \forall \;\; a,b = 1,2,3,.. \end{aligned} \tag{36}$$

Equations (35) and (36) have to be identical. This implies the following relation must exist between the $[e]$ and $[g]$ matrices.

$$\frac{1}{b}\left[ e^{(a,b-1)} \right] = \frac{1}{a}\left[ g^{(a-1,b)} \right] \qquad \forall \;\; a,b = 1,2,3,.. \tag{37}$$

Equation (37) physically means that when $\boldsymbol{f}_{x1}$ and $\boldsymbol{m}_{xd1}$ are applied together on the spatial beam, the work done by $\boldsymbol{f}_{x1}$ due to the $u_x$ displacement produced by $\boldsymbol{m}_{xd1}$ is equal to the work done by $\boldsymbol{m}_{xd1}$ due to the $\theta_{xd1}$ displacement produced by $\boldsymbol{f}_{x1}$. This is simply a manifestation of Maxwell's reciprocity theorem. For a uniform thickness spatial beam, Eq. (37) is easily verified using reference [3].

Using Eqs.(25), (35) and (37), matrices $[g^{(a,b)}]$, $[e^{(a,b)}]$ and $[v^{(a,b)}]$ can all be expressed in terms of $[k^{(a,b)}]$.

$$\left[v^{(a,b)}\right]=(1-a-b)\left[k^{(a,b)}\right] \quad \forall \quad a,b=0,1,2,3,....$$
$$\left[g^{(a,b)}\right]=-\frac{a+1}{2}\left[k^{(a+1,b)}\right] \quad \forall \quad a,b=0,1,2,3,....$$
$$\left[e^{(0,0)}\right]=-\frac{1}{2}\left(\left[k^{(0,1)}\right]+\left[H_7\right]\right) \tag{38}$$
$$\left[e^{(a,b)}\right]=$$
$$-\frac{b+1}{2}\left[k^{(a,b+1)}\right], \forall \quad a,b=0,1,2,.. \text{ except } a=b=0$$

Equation (38) forms the fundamental relations between the beam characteristic coefficients and shows that all the beam characteristic coefficients can be easily obtained from the solution of the bending load-displacement equation (20) only. Therefore, for any beam shape, as long as it is slender and its cross-section is bisymmetric, one only needs to solve the differential equation related to bending, Eq.(17) either analytically or numerically to obtain the [*H*] matrices. Explicit solving of the nonlinear equations in Eq.(18) is no longer required to complete the SBCM.

The formulation of an initially tilted spatial beam flexure and variable cross-section spatial beam flexure can be combined, by noticing that the effect of the initial tilt is purely geometric in nature. As a result, the tilt angles $\beta$ and $\gamma$, do not appear in the strain energy expression, Eq.(15). Therefore the load displacement and constraint relation for a tilt spatial beam with variable but bisymmetric cross-section can be written as:

$$\begin{Bmatrix} \boldsymbol{f_{y1}} & \boldsymbol{m_{z1}} & \boldsymbol{f_{z1}} & \boldsymbol{m_{y1}} \end{Bmatrix}$$
$$=\sum_{n=0}^{\infty}\sum_{i=0}^{n}\boldsymbol{f}_{x1}^{n-i}\boldsymbol{m}_{xd1}^{i}\left[k^{(n-i,i)}\right]\begin{Bmatrix} u_{y1} & u'_{y1} & u_{z1} & -u'_{z1} \end{Bmatrix} \tag{39}$$
$$+\boldsymbol{m}_{xd1}\begin{Bmatrix} 0 & -\beta & 0 & \gamma \end{Bmatrix}^T+\boldsymbol{f}_{x1}\begin{Bmatrix} \gamma & 0 & -\beta & 0 \end{Bmatrix}^T$$

$$u_{x1}=-\gamma u_{y1}+\beta u_{z1}+\frac{\boldsymbol{f_{x1}}}{\bar{k}_{33}}-\frac{\boldsymbol{m_{xd1}^2}}{\bar{k}_{44}^2\bar{k}_{33}}$$
$$-\sum_{n=0}^{\infty}\sum_{i=0}^{n}\frac{n-i+1}{2}\boldsymbol{f}_{x1}^{n-i}\boldsymbol{m}_{xd1}^{i}\begin{Bmatrix} u_{y1} \\ u'_{y1} \\ u_{z1} \\ -u'_{z1} \end{Bmatrix}^T\left[k^{(n-i+1,i)}\right]\begin{Bmatrix} u_{y1} \\ u'_{y1} \\ u_{z1} \\ -u'_{z1} \end{Bmatrix} \tag{40}$$

$$\theta_{xd1}=u'_{z1}\gamma+\frac{\boldsymbol{m_{xd1}}}{\bar{k}_{\theta}}-\frac{2\boldsymbol{m_{xd1}}\boldsymbol{f_{x1}}}{\bar{k}_x\bar{k}_{\theta}^2}$$
$$-\frac{1}{2}\begin{Bmatrix} u_{y1} \\ u'_{y1} \\ u_{z1} \\ -u'_{z1} \end{Bmatrix}^T\left(\begin{matrix}\left[H_7\right] \\ +\sum_{n=0}^{\infty}\sum_{i=0}^{n}(i+1)\,\boldsymbol{f}_{x1}^{n-i}\boldsymbol{m}_{xd1}^{i}\left[k^{(n-i,i+1)}\right]\end{matrix}\right)\begin{Bmatrix} u_{y1} \\ u'_{y1} \\ u_{z1} \\ -u'_{z1} \end{Bmatrix} \tag{41}$$

The corresponding strain energy is:

$$v = \frac{\boldsymbol{m}_{xd1}^2}{2\bar{k}_\theta} + \frac{\boldsymbol{f}_{x1}^2}{2\bar{k}_x} - \frac{2\boldsymbol{m}_{xd1}^2 \boldsymbol{f}_{x1}}{\bar{k}_x \bar{k}_\theta^2}$$
$$+ \frac{1}{2} \begin{Bmatrix} u_{y1} \\ u'_{y1} \\ u_{z1} \\ -u'_{z1} \end{Bmatrix}^T \left( \begin{bmatrix} k^{(0,0)} \end{bmatrix} + \sum_{n=1}^{\infty} \sum_{i=0}^{n} (1-n-2i)\, \boldsymbol{f}_{x1}^{n-i} \boldsymbol{m}_{xd1}^{i} \left[ k^{(n-i,i)} \right] \right) \begin{Bmatrix} u_{y1} \\ u'_{y1} \\ u_{z1} \\ -u'_{z1} \end{Bmatrix} \tag{42}$$

The SBCM given in Eqs. (39) to (42) represent the model of a beam that has arbitrarily varying shape as well as small but otherwise arbitrary initial tilts. As will be shown in section 4, this generalized form of SBCM allows a closed-form performance characterization of the stiffness and error motion characteristics of flexure mechanisms that use bisymmetric spatial beam flexure elements of varying cross-section as a building block. Furthermore, the effect of misalignment of the flexure elements can be also be studied in closed-form without transformations from local to global co-ordinate frame.

## 4. CASE-STUDY: MULTI-LEGGED TABLE FLEXURE MECHANISM

In this section, using the strain energy of the initially-tilted, slender and bisymmetric but otherwise arbitrarily shaped, spatial beam flexure derived in the previous section, the principle of virtual work will be used to formulate the parametric closed-form nonlinear load-displacement relations of a multi-legged table flexure mechanism, shown in Figure 2. Let the legs be identical in shape and be numbered 1 through n. Also let us assume that the motion stage is initially horizontal and at a height L. The location of the $i^{th}$ beam is given by the normalized (with respect to L) co-ordinates ($y_i$, $z_i$) in the global co-ordinate system X-Y-Z as shown in Figure 2. Also let each leg be tilted with respect to X-Y-Z by tilt angles $\beta_i$ and $\gamma_i$ in the same sense as shown in section 2. The tilt angles $\beta_i$ and $\gamma_i$ are assumed to be within -0.1 and 0.1 radians. For simplicity, it is assumed that each of the principle axes of moment of area of the cross-sections of all the spatial beam flexures align with the global coordinate axis i.e $\alpha_i = 0$ . If this was not the case, the beam characteristic [H] matrices will need to be modified as per Eq. (16). Although, such a case does not increase the overall mathematical complexity, it is not considered here. Finally let the normalized displacement of the motion stage be described by $\{u_{xs},\ u_{ys},\ u_{zs},\ \theta_{xs},\ \theta_{ys}$ and $\theta_{zs}\}$.

In the displacement range of interest, the individual translational end-displacements of each beam can be approximately expressed in terms of the stage displacement as given in Eq.(43). These relations use second order approximations which are based on preliminary FEA experiments of table flexure mechanism with 3 or more legs that

show, for normalized planar translation and rotation ($u_{ys}$, $u_{zs}$, $\theta_{xs}$) of *0.1* and *0.1* radians, respectively, the out of plane translation $u_{xs}$ and rotations, $\theta_{ys}$ and $\theta_{zs}$, are of the order of 0.01. Furthermore the rigidity of the motion stage constrains the rotation of all the beams to be equal as shown in Eq.(44).

$$\begin{aligned} &u_{x,i} \approx u_{xs} - y_i\left(\theta_{zs} - \theta_{xs}\theta_{ys}\right) + z_i\left(\theta_{ys} + \theta_{xs}\theta_{zs}\right); \\ &u_{y,i} \approx u_{ys} - \frac{1}{2}y_i\theta_{xs}^2 - z_i\theta_{xs};\ u_{z,i} \approx u_{zs} - \frac{1}{2}z_i\theta_{xs}^2 + y_i\theta_{xs} \end{aligned} \tag{43}$$

$$\theta_{x,i} = \theta_{xs},\ \theta_{y,i} = \theta_{ys},\ \theta_{z,i} = \theta_{zs} \tag{44}$$

The truncated strain energy and constraint equations of the tilted, general, spatial beam model, used in this case, are given in Eq.(45)-(47). The trapeze effect is dropped here assuming that axial load $|\boldsymbol{f}_x|$ for any beam is limited to approximately 5 in order to keep a sufficient safety margin from buckling which occurs at $\boldsymbol{f}_x = \pi^2$. Furthermore, since the terms containing products of $\boldsymbol{f}_{x1}$ and $\boldsymbol{m}_{xd1}$ have small coefficients in comparison to the linear, kinematic and elastokinematic terms, they are dropped in this analysis. Finally, the elastokinematic effect in torsion is dropped because the torsional stiffness of the stage is dominated by the elastic torsional stiffness and spacing of the beams. Overall this model captures the load-displacement relations of the table flexure mechanism by considering the linear elastic effect, the nonlinear kinematic in torsional and axial stretching direction and elastokinematic effects in the axial stretching directions for the bisymmetric spatial beam flexures with tilts and varying cross-section that are its building blocks.

$$v_i = \frac{\boldsymbol{m}_{xd1,i}^2}{2\bar{k}_{44}} + \frac{\boldsymbol{f}_{x1,i}^2}{2\bar{k}_{33}} + \frac{1}{2}\begin{Bmatrix} u_{y1,i} \\ \theta_{z1,i} \\ u_{z1,i} \\ \theta_{y1,i} \end{Bmatrix}^T \left(\left[k^{(0,0)}\right] - \boldsymbol{f}_{x1}^2\left[k^{(2,0)}\right]\right)\begin{Bmatrix} u_{y1,i} \\ \theta_{z1,i} \\ u_{z1,i} \\ \theta_{y1,i} \end{Bmatrix} \tag{45}$$

$$\begin{aligned} u_{x1,i} = &-\gamma_i u_{y1,i} + \beta_i u_{z1,i} + \frac{\boldsymbol{f}_{x1,i}}{\bar{k}_{33}} \\ &-\frac{1}{2}\begin{Bmatrix} u_{y1,i} \\ \theta_{z1,i} \\ u_{z1,i} \\ \theta_{y1,i} \end{Bmatrix}^T \left(\left[k^{(1,0)}\right] + 2\,\boldsymbol{f}_{x1,i}\left[k^{(2,0)}\right]\right)\begin{Bmatrix} u_{y1,i} \\ \theta_{z1,i} \\ u_{z1,i} \\ \theta_{y1,i} \end{Bmatrix} \end{aligned} \tag{46}$$

$$\theta_{xd1,i} = -\theta_{y,i}\gamma_i + \frac{\boldsymbol{m_{xd1,i}}}{\bar{k}_{44}} - \frac{1}{2}\begin{Bmatrix} u_{y1,i} \\ \theta_{z1,i} \\ u_{z1,i} \\ \theta_{y1,i} \end{Bmatrix}^T \left( \left[ k^{(0,1)} \right] + \left[ H_7 \right] \right) \begin{Bmatrix} u_{y1,i} \\ \theta_{z1,i} \\ u_{z1,i} \\ \theta_{y1,i} \end{Bmatrix} \tag{47}$$

The values of $\boldsymbol{f_{x,i}}$ and $\boldsymbol{m_{xd,i}}$ are solved from Eq.(46) and (47), and substituted in the strain energy expression given in Eq.(45). The total strain energy, obtained by summing the strain energy for all the beams, is given below in terms of the displacements of the rigid motion stage.

$$\begin{aligned} v = \sum_i v_i = {} & \frac{1}{2}\sum_i \begin{Bmatrix} u_{y1,i} \\ \theta_{z1,i} \\ u_{z1,i} \\ \theta_{y1,i} \end{Bmatrix} \left[ k^{0,0} \right] \begin{Bmatrix} u_{y1,i} \\ \theta_{z1,i} \\ u_{z1,i} \\ \theta_{y1,i} \end{Bmatrix}^T \\ & + \frac{1}{2}\sum_i \frac{\left\{ u_{x,i} + \gamma_i u_{y,i} - \beta_i u_{z,i} + \frac{1}{2}\begin{Bmatrix} u_{y1,i} \\ \theta_{z1,i} \\ u_{z1,i} \\ \theta_{y1,i} \end{Bmatrix} \left[ k^{1,0} \right] \begin{Bmatrix} u_{y1,i} \\ \theta_{z1,i} \\ u_{z1,i} \\ \theta_{y1,i} \end{Bmatrix}^T \right\}^2}{\left( \frac{1}{\bar{k}_{33}} - \begin{Bmatrix} u_{y1,i} \\ \theta_{z1,i} \\ u_{z1,i} \\ \theta_{y1,i} \end{Bmatrix} \left[ k^{2,0} \right] \begin{Bmatrix} u_{y1,i} \\ \theta_{z1,i} \\ u_{z1,i} \\ \theta_{y1,i} \end{Bmatrix}^T \right)} \\ & + \frac{1}{2}\bar{k}_{44}\sum_i \left\{ \theta_{xds} + \gamma_i \theta_{ys} + \frac{1}{2}\begin{Bmatrix} u_{y1,i} \\ \theta_{z1,i} \\ u_{z1,i} \\ \theta_{y1,i} \end{Bmatrix} \left( \left[ k^{0,1} \right] + \left[ H_7 \right] \right) \begin{Bmatrix} u_{y1,i} \\ \theta_{z1,i} \\ u_{z1,i} \\ \theta_{y1,i} \end{Bmatrix}^T \right\}^2 \end{aligned} \tag{48}$$

The principle of Virtual Work given in Eq.(24) is applied to the multi-beam table flexure mechanism next. By is a substituting $\theta_{ys} = -u'_{zs}$ and $\theta_{zs} = u'_{ys}$ the modified expression of PVW becomes

$$\begin{aligned} \delta v = {} & \boldsymbol{f_{xs}}\delta u_{xs} + \boldsymbol{f_{ys}}\delta u_{ys} + \boldsymbol{f_{zs}}\delta u_{zs} + \boldsymbol{m_{xds}}\delta\theta_{xds} \\ & + \boldsymbol{m_{ys}}\delta\theta_{ys} + \left( \boldsymbol{m_{zs}} + \boldsymbol{m_{xds}}\theta_{ys} \right)\delta\theta_{zs} \end{aligned} \tag{49}$$

where $\boldsymbol{m_{xds}} \triangleq \boldsymbol{m_{xs}} + \theta_{zs}\boldsymbol{m_{ys}} - \theta_{ys}\boldsymbol{m_{zs}}$

We recognize that the virtual displacements $\delta u_{xs}$, $\delta u_{ys}$, $\delta u_{zs}$, $\delta\theta_{xds}$, $\delta\theta_{ys}$, $\delta\theta_{zs}$ are arbitrary quantities and their respective coefficients from both sides of Eq.(49) should be identical. Using Eqs.(43), (44) and (48), the load-displacement relations can be derived as follows:

$$\begin{Bmatrix} \boldsymbol{f}_{ys} \\ \boldsymbol{m}_{zs} \\ \boldsymbol{f}_{zs} \\ \boldsymbol{m}_{ys} \end{Bmatrix} = \left( n\left[k^{0,0}\right] + \left[k^{1,0}\right]\boldsymbol{f}_{xs} - \boldsymbol{m}_{xds}\left[H_7\right]\right) \begin{Bmatrix} u_{ys} \\ \theta_{zs} \\ u_{zs} \\ \theta_{ys} \end{Bmatrix} \tag{50}$$

$$+ \sum_i \left[k^{0,0}\right]\{r_i\} + \sum_i \left[k^{1,0}\right]\frac{\{a_i\}}{\{b_i\}}\{r_i\}$$

$$+ \sum_i \left[k^{2,0}\right]\frac{\{a_i\}^2}{\{b_i\}^2}\left(\{u_{ys} \quad \theta_{zs} \quad u_{zs} \quad \theta_{ys}\}^T + \{r_i\}\right)$$

$$+ \bar{k}_{44}\sum_i \left(\left[k^{0,1}\right] + \left[H_7\right]\right)\{c_i\}\left(\{u_{ys} \quad \theta_{zs} \quad u_{zs} \quad \theta_{ys}\}^T + \{r_i\}\right)$$

$$+ \begin{Bmatrix} \sum_i \frac{\{a_i\}\gamma_i}{\{b_i\}} \\ \sum_i \frac{\{a_i\}(-y_i + \theta_{xs} z_i)}{\{b_i\}} \\ -\sum_i \frac{\{a_i\}\beta_i}{\{b_i\}} \\ \sum_i \gamma_i \{c_i\} + \frac{\{a_i\}(z_i + \theta_{xs} y_i)}{\{b_i\}} \end{Bmatrix}$$

$$\boldsymbol{f}_{xs} = \sum_i \frac{\{a_i\}}{\{b_i\}} \tag{51}$$

$$\boldsymbol{m}_{xds} = \bar{k}_{44}\sum_i \{c_i\}\left[1 + \{s_i\}\left(\left[k^{0,1}\right] + \left[H_7\right]\right)\left(\begin{Bmatrix} u_{ys} \\ \theta_{zs} \\ u_{zs} \\ \theta_{ys} \end{Bmatrix} + \{r_i\}\right)\right]$$

$$+ \sum_i \{s_i\}\left[k^{0,0}\right]\left(\begin{Bmatrix} u_{ys} \\ \theta_{zs} \\ u_{zs} \\ \theta_{ys} \end{Bmatrix} + \{r_i\}\right)$$

$$+ \sum_i \frac{\{a_i\}}{\{b_i\}}\left[\begin{matrix} y_i\theta_{ys} + z_i\theta_{zs} + \{s_i\}\left[k^{1,0}\right]\left(\begin{Bmatrix} u_{ys} \\ \theta_{zs} \\ u_{zs} \\ \theta_{ys} \end{Bmatrix} + \{r_i\}\right) \\ -\gamma_i\left(y_i\theta_{xs} + z_i\right) + \beta_i\left(z_i\theta_{xs} - y_i\right) \end{matrix}\right] \tag{52}$$

$$+ \sum_i \frac{\{a_i\}^2}{\{b_i\}^2}\{s_i\}\left[k^{2,0}\right]\left(\{u_{ys} \quad \theta_{zs} \quad u_{zs} \quad \theta_{ys}\}^T + \{r_i\}\right)$$

where $\{a_i\} \triangleq \left\{ u_{x,i} + \gamma_i u_{y,i} - \beta_i u_{z,i} + \frac{1}{2} \begin{Bmatrix} u_{y1,i} \\ \theta_{z1,i} \\ u_{z1,i} \\ \theta_{y1,i} \end{Bmatrix}^T \left[k^{1,0}\right] \begin{Bmatrix} u_{y1,i} \\ \theta_{z1,i} \\ u_{z1,i} \\ \theta_{y1,i} \end{Bmatrix} \right\}$,

$\{b_i\} \triangleq \left( \frac{1}{\bar{k}_{33}} - \begin{Bmatrix} u_{y1,i} \\ \theta_{z1,i} \\ u_{z1,i} \\ \theta_{y1,i} \end{Bmatrix}^T \left[k^{2,0}\right] \begin{Bmatrix} u_{y1,i} \\ \theta_{z1,i} \\ u_{z1,i} \\ \theta_{y1,i} \end{Bmatrix} \right)$,

$\{c_i\} \triangleq \left\{ \theta_{xds} + \gamma_i \theta_{ys} + \frac{1}{2} \begin{Bmatrix} u_{y1,i} \\ \theta_{z1,i} \\ u_{z1,i} \\ \theta_{y1,i} \end{Bmatrix}^T \left( \left[k^{0,1}\right] + \left[H_7\right] \right) \begin{Bmatrix} u_{y1,i} \\ \theta_{z1,i} \\ u_{z1,i} \\ \theta_{y1,i} \end{Bmatrix} \right\}$

$\{r_i\} \triangleq \left\{ -\frac{1}{2} y_i \theta_{xs}^2 - z_i \theta_{xs} \quad 0 \quad -\frac{1}{2} z_i \theta_{xs}^2 + y_i \theta_{xs} \quad 0 \right\}^T$,

$\{s_i\} \triangleq \{ -y_i \theta_{xs} - z_i \quad 0 \quad -z_i \theta_{xs} + y_i \quad 0 \}$

Equations (50)-(52) express the externally applied loads completely in terms of the displacements of the motion stage. This analytical model is valid for any number of beams, any beam spacing, and small (~0.1 radians) but arbitrary tilts at each beam, for a displacement range of $u_{ys}$, $u_{zs}$, $\theta_{xds}$ within ± 0.1 and $u_{xs}$, $\theta_{ys}$, $\theta_{zs}$ within ±0.01. Furthermore, these equations are also valid if instead of using a prismatic spatial beam flexure as legs, some other bisymmetric spatial beam flexure with varying cross-section is used. For validation using FEA, a specific case of the n-legged table is considered with all the beam flexures perfectly vertical and placed symmetrically about the center axis on a circle of radius $p \times L$. This implies the following summations are zero.

$$\sum_i y_i = \sum_i z_i = \sum_i y_i z_i = 0 \tag{53}$$

Using this relation, the in-plane load displacement relations can be simplified to

$$\boldsymbol{f}_{ys} \approx \left( 12n + \frac{6}{5} \boldsymbol{f}_{xs} \right) u_{ys} - \frac{18\theta_{xs}^2}{25} \boldsymbol{m}_{zs} - \frac{6\theta_{xs}}{5} \boldsymbol{m}_{ys} \tag{54}$$

$$\boldsymbol{f}_{zs} \approx \left( 12n + \frac{6}{5} \boldsymbol{f}_{xs} \right) u_{zs} + \frac{18\theta_{xs}^2}{25} \boldsymbol{m}_{ys} - \frac{6\theta_{xs}}{5} \boldsymbol{m}_{zs} \tag{55}$$

$$\boldsymbol{m}_{xs} \approx \left( n\bar{k}_{44} + 12np^2 + \frac{6}{5} p^2 \boldsymbol{f}_{xs} + \frac{3}{25} \left( \boldsymbol{m}_{ys} u_{zs} - \boldsymbol{m}_{zs} u_{ys} \right) \right) \theta_{xs} - \frac{6u_{ys} \boldsymbol{m}_{ys}}{5} - \frac{6u_{zs} \boldsymbol{m}_{zs}}{5} \tag{56}$$

Here the summation terms are eliminated using the out-of plane load-displacement relations in Eq.(50) and (51) associated with $u_{xs}$, $\theta_{ys}$ and $\theta_{zs}$.

The in-plane displacement directions and in-plane rotation experience nonlinear stiffening or softening as shown in equations (54)-(56). The out-of-plane force $\boldsymbol{f}_{xs}$ produces a load stiffening effect in linearly changes the stiffness of in-plane translations, $u_{ys}$ and $u_{zs}$. Although this effect is mathematically linear, it is called a nonlinear effect here because it arises from considering nonlinear geometric nature of the problem. This effect is verified for a three legged table flexure with $p = 2/\sqrt{3}$ against FEA in Figure 5(i) using BEAM188 element in ANSYS with geometric nonlinearities turned on (Command: NLGEOM, ON). The discrepancy between FEA and the SBCM model is less than 3% for the given range of displacements. It should be noted that these relations for 3 legged table mechanism is consistent with the results provided in reference [14].

The in-plane translations, $u_{ys}$ and $u_{zs}$ are also effected by out-of-plane moments $\boldsymbol{m}_{ys}$ and $\boldsymbol{m}_{zs}$ in the presence in in-plane rotation $\theta_{xs}$. These error motions are verified against FEA for the same table flexure in Figure 5(ii) and (iii). The discrepancy between FEA and the SBCM model in Figure 5(ii) is less than 5% while in Figure 5(iii) the discrepancy is 30% for extreme values of the end-displacements. This is because the small effect shown in Figure 5(iii) is a second order effect and suffers from the second order approximations.

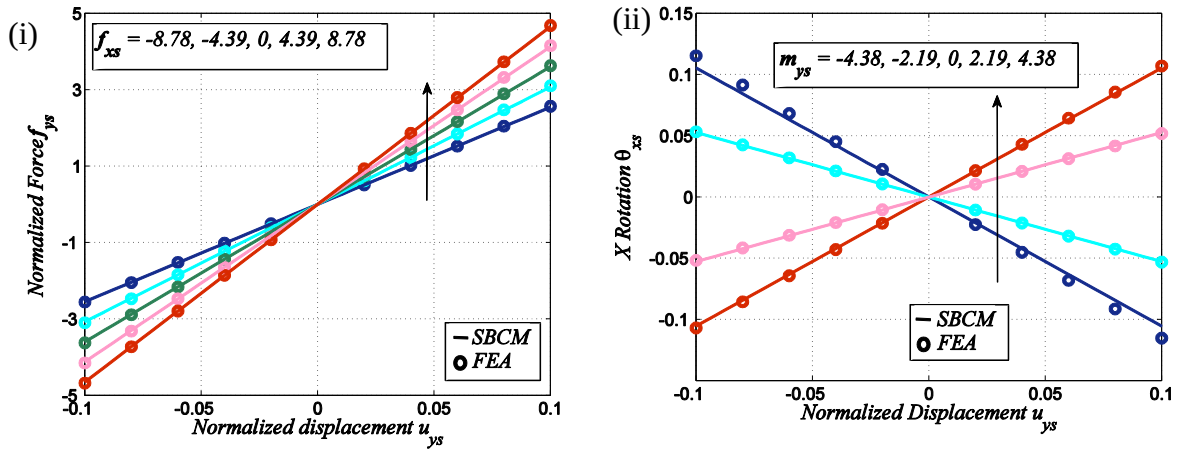

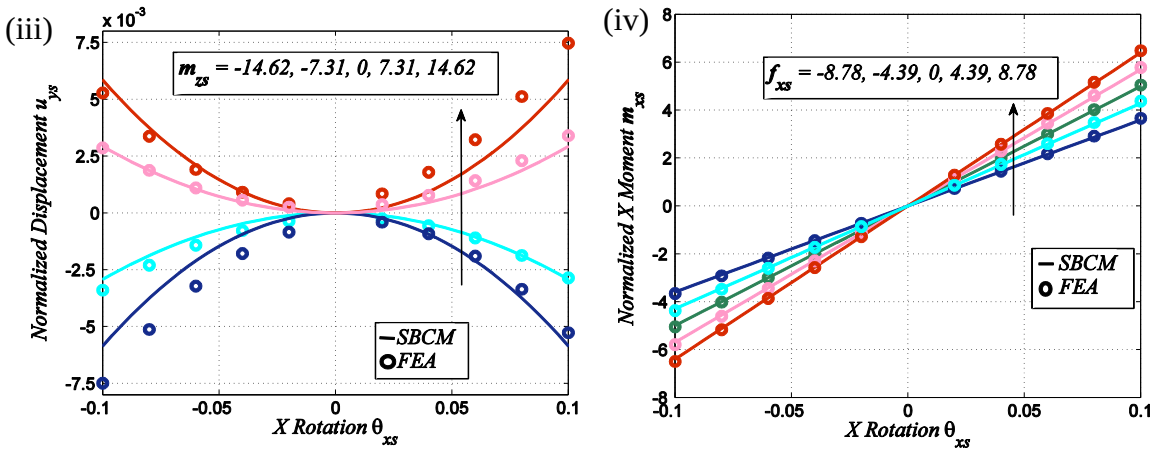


*Figure 5:(i) Load stiffening during in-plane translation along y, (ii) In-plane translation along y due to in-plane rotation in the presence of* $\boldsymbol{m}_{ys}$*, (iii) In-plane translation along y due to in-plane rotation in the presence of* $\boldsymbol{m}_{zs}$*, (iv) Load stiffening during in-plane rotation due to x*

Similar to the in-plane translations, the in-plane rotation $\theta_{xs}$ also experiences the load-stiffening effect due to $\boldsymbol{f}_{xs}$ which is verified in Figure 5(iv) as well as error motions due to in-plane translations and out-of-plane moments as verified in Figure 5(iv). In either case the discrepancy between FEA and the SBCM model is less than 5% for the given displacement ranges.

The load-displacement relations for the out-of-plane displacements $u_{xs}$, $\theta_{ys}$ and $\theta_{zs}$, which are typically the stiff directions of this mechanism, can also be solved from Eqs. (50)-(51). After using Eq.(53) for simplification, these three equations appear as three linearly coupled equations which can be solved using linear algebra.

$$\begin{Bmatrix} \boldsymbol{f}_{xs} + \frac{6}{5} p\theta_{xs} d_7 \sqrt{u_{ys}^2 + u_{zs}^2} \\ \boldsymbol{m}_{ys} - \left(6n + \frac{1}{10}\boldsymbol{f}_{xs}\right) u_{zs} - n\bar{k}_{44}\theta_{xs} u_{ys} + \frac{6}{5} p\theta_{xs} d_8 \sqrt{u_{ys}^2 + u_{zs}^2} \\ \boldsymbol{m}_{zs} + \left(6n + \frac{1}{10}\boldsymbol{f}_{xs}\right) u_{ys} - n\bar{k}_{44}\theta_{xs} u_{zs} + \frac{6}{5} p\theta_{xs} d_9 \sqrt{u_{ys}^2 + u_{zs}^2} \end{Bmatrix} \tag{57}$$

$$= \left[k_{stiff}\right] \begin{Bmatrix} u_{xs} + \frac{3}{5}\left(u_{ys}^2 + u_{zs}^2 + p^2\theta_{xs}^2\right) \\ \theta_{ys} \\ \theta_{zs} \end{Bmatrix}$$

where $\left[k_{stiff}\right] \triangleq$

$$\begin{bmatrix} d_1 & p\left(d_3+\theta_{xs}d_2\right) & -p\left(d_2-\theta_{xs}d_3\right) \\ p\begin{pmatrix} d_3+ \\ 1.1\theta_{xs}d_2 \end{pmatrix} & 4n+\frac{2}{15}\boldsymbol{f}_{xs}+p^2d_6 \\ & +p^2\begin{pmatrix} 2.1\theta_{xs}d_4 \\ +1.1\theta_{xs}^2d_5 \end{pmatrix} & -p^2\begin{pmatrix} d_4 \\ -\theta_{xs}d_6 \\ +1.1\theta_{xs}d_5 \end{pmatrix} \\ p\begin{pmatrix} -d_2+ \\ 1.1\theta_{xs}d_3 \end{pmatrix} & -p^2\begin{pmatrix} d_4+\theta_{xs}d_5 \\ -1.1\theta_{xs}d_6 \end{pmatrix} & 4n+\frac{2}{15}\boldsymbol{f}_{xs} \\ & & +p^2\begin{pmatrix} d_5-2.1\theta_{xs}d_4 \\ +1.1\theta_{xs}^2 \end{pmatrix} \end{bmatrix}$$

$$\psi_i \triangleq \tan^{-1}\left(\frac{u_{zs}}{u_{ys}}\right)+\frac{\theta_{xs}}{2}-\tan^{-1}\left(\frac{y_i}{z_i}\right),$$

$$d_{0,i} \triangleq \frac{1}{\bar{k}_{33}}+$$

$$\frac{1}{700}\left(u_{ys}^2+u_{zs}^2+p^2\theta_{xs}^2-2p\theta_{xs}\sqrt{u_{ys}^2+u_{zs}^2}\cos\left(\psi_i\right)\right)$$

$$d_1 \triangleq \sum_i \frac{1}{a_{0,i}}, d_2 \triangleq \sum_i \frac{y_i}{pa_{0,i}},\ d_3 \triangleq \sum_i \frac{z_i}{pa_{0,i}}, d_4 \triangleq \sum_i \frac{y_iz_i}{p^2a_{0,i}}$$

$$d_5 \triangleq \sum_i \frac{y_i^2}{p^2a_{0,i}},\ \ d_6 \triangleq \sum_i \frac{z_i^2}{p^2a_{0,i}},\ \ d_7 \triangleq \sum_i \frac{\cos\left(\psi_i\right)}{a_{0,i}},$$

$$d_8 \triangleq \sum_i \frac{y_i\cos\left(\psi_i\right)}{pa_{0,i}},\ \ d_9 \triangleq \sum_i \frac{z_i\cos\left(\psi_i\right)}{pa_{0,i}}$$

Although the out-of-plane motions in Eq. (57) are related to any general loading and general in-plane displacement in a highly complicated manner, in the cases when either in-plane rotation is zero ($\theta_{xs}=0$) or in-plane translation is zero ($u_{ys}=u_{zs}=0$), Eq. (57) may be considerably simplified because the denominator $a_{0,i}$ becomes constant while $a_2$, $a_3$, and $a_4$ all become zero.

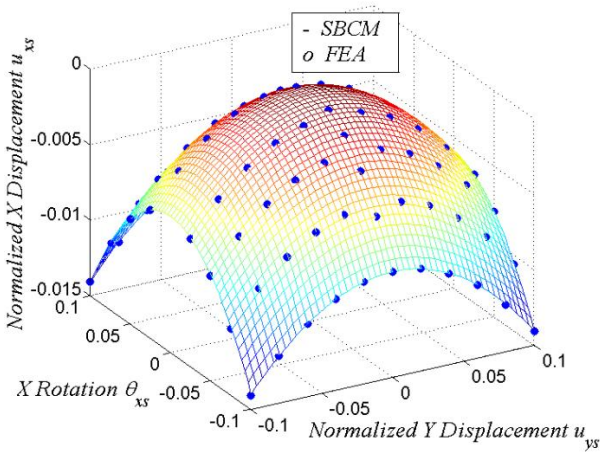


*Figure 6: Parasitic Error motion in $u_{xs}$ due to $u_{ys}$ and $\theta_{xs}$*

Validation of error-motions in $u_{xs}$ due to in-plane translation $u_{ys}$ and in-plane rotation $\theta_{xs}$ in the absence of out-of-plane loads $\boldsymbol{f}_{xs}$, $\boldsymbol{m}_{ys}$ and $\boldsymbol{m}_{zs}$ for a 3 legged table mechanism is shown in Figure 6. The discrepancy between the FEA and the SBCM is less than 4% for the given displacement range. As can be seen in this figure, $u_{xs}$ has a quadratic dependence on both in-plane translation $u_{ys}$ and $u_{zs}$ as well as on in-plane rotation $\theta_{xs}$. The stiffness in $u_{xs}$, $\theta_{ys}$ and $\theta_{zs}$ is captured in the $[k_{stiff}]$ matrix. This matrix shows that the out-of-plane stiffness drops with $u_{ys}$, $u_{zs}$ and $\theta_{xs}$ in a quadratic manner due to the elastokinematic effect reducing the axial stiffness of each leg of the table flexure.This example shows that once a consistent SBCM energy formulation has been derived, the use of energy methods considerably reduces the mathematical complexity in the analysis of increasingly sophisticated flexure mechanisms. The above procedure is relatively independent of the number of beams chosen or the shapes of the individual beams or the parallelism between the beams as long as the strain energy associated with each beam is accounted for correctly. Given the closed-form nature of the final expression design insights in terms of how many legs to use, type of legs to use and spacing between the legs can be determined in a relative simple manner.

The limitation of this approach mainly arises from the second order approximations done to derive Eq. (2)-(5). Since this assumption is suitable when the Euler angles of the deformed beam from the undeformed and untilted co-ordinate axes X-Y-Z are within 0.1 radians, the accuracy drops when the tilt angles become large. It is found that when tilt angles $\beta_i$ and $\gamma_i$ are close to 0.1 radians, the errors in the SBCM load-displacement relations are approximately doubled for a translational and angular displacement range of 0.1L and 0.1 radians.

## 5. CONCLUSION

This paper provides a generalized, closed-form and parametric mathematical model of any spatial beam with bisymmetric cross-section that accurately captures the non-linear load-displacement relations of the spatial beam for intermediate range of end-displacements. The model, referred to as the spatial beam constraint model (SBCM) not only accommodates small initial tilts with respect to a predefined axial direction, but also cross-sectional variations of the beam along its length.

The key contribution of the SBCM is its highly generalized non-linear strain energy and constraint equations which enable the use of energy methods, such as the principle of virtual work, in analyzing flexure mechanisms subjected to spatial end-loads. In parallel configuration of flexure elements, the SBCM shows its versatility in capturing the stiffness and error-motion characteristics in a closed-form for an arbitrary number of flexure elements with arbitrary spacing, which makes handling multiple flexure elements relatively easy. With these results, design decisions regarding the number of flexure elements to use or the spacing between the flexure elements in the flexure mechanism can be taken in an informed and deterministic manner.

## REFERENCES


[1] S. T. Smith, 2000, *Flexures: Elements of Elastic Mechanisms*. New York, NY: Gordon and Breach Science Publishers.

[2] R. V. Jones, 1988, *Instruments and Experiences: Papers on Measurement and Instrument Design*. New York, NY: John Wiley & Sons.

[3] S. Sen and S. Awtar, 2013, "A Closed-Form Non-Linear Model for the Constraint Characteristics of Symmetric Spatial Beams," *ASME Journal of Mechanical Design,* Vol. 135, pp 031003-1 - 031003-11

[4] N. O. Rasmussen, J. W. Wittwer, R. H. Todd, L. L. Howell, and S. P. Magleby, 2006, "A 3D Pseudo-Rigid-Body Model for Large Spatial Deflections of Rectangular Cantilever Beams," in *International Design Engineering Technical Conferences & Computers and Information in Engineering Conference*, Philadelphia, PA.

[5] I. A. Ramirez and C. Lusk, 2011, "Spatial-beam large-deflection equations and pseudo-rigid body model for axisymmetric cantilever beams," in *Proc. IDETC/CIE 2011*, Washington D. C., Paper # 47389.

[6] T. R. Tauchert, 1974, *Energy Principles in Structural Mechanics*. New York, NY: McGraw-Hill.

[7] K. S. Chen, D. L. Trumper, and S. T. Smith, 2002, "Design and control for an electromagnetically driven X–Y–θ stage," *Precision Engineering*, vol. 26, pp. 355-369.

[8] H. D. Samuel and N. S. Sergio, "Compliant assembly system," US Patent, 1979.

[9] X. L. Ding and J. S. Dai, 2006, "Characteristic Equation-Based Dynamics Analysis of Vibratory Bowl Feeders with Three Spatial Compliant Legs," *IEEE Transactions on Robotics and Automation*, vol. 5, pp. 164-175.

[10] S. Awtar., T. T. Trutna, J. M. Nielsen, R. Abani, and J. D. Geiger, 2010, "FlexDex: A Minimally Invasive Surgical Tool with Enhanced Dexterity and Intuitive Actuation," *ASME Journal of Medical Devices*, vol. 4,

[11] G. Hao and X. Kong, 2012, "A Novel Large-Range XY Compliant Parallel Manipulator With Enhanced Out-of-Plane Stiffness," *ASME Journal of Mechanical Design*, vol. 134,

[12] S. Awtar and S. Alexander H, 2007, "Constraint-based design of parallel kinematic XY flexure mechanisms," *ASME Journal of Mechanical Design*, vol. 129, pp. 816-830.

[13] C. J. Kim, Y. M. Moon, and S. Kota, 2008, "A Building Block Approach to the Conceptual Synthesis of Compliant Mechanisms (a) Double three-blade module (b) Double four-blade module Motion stage Utilizing Compliance and Stiffness Ellipsoids," *Journal of Mechanical Design*, vol. 130, pp. 022308.1-022308.11.

[14] G. Hao, X. Kong, and R. L. Reuben, 2011, "A nonlinear analysis of spatial compliant parallel modules: Multi-beam modules," *Mechanism and Machine Theory*, vol. 46, pp. 680-706.

[15] S. Timoshenko and J. N. Goodier, 1969, *Theory of Elastisity*. New York, NY: McGraw-Hill.

[16] M. R. M. C. DaSilva, 1988, "Non-Linear Flexural-flexural-torsional-Extensional Dynamics of Beams-I. Formulation," *International Journal of Solid Structures*, vol. 24, pp. 1225-1234.

[17] S. Awtar, A. H. Slocum, and E. Sevincer, 2006, "Characteristics of Beam-based Flexure Modules," *Journal of Mechanical Design*, vol. 129, pp. 625-639.

List of figure captions

1. Figure 1: Spatial Beam Flexure, Undeformed and Deformed Configurations
2. Figure 2: A 3-DoF Spatial Flexure Mechanism
3. Figure 3: (a) Tilted Spatial Beam deformation (b) Relating the orientation of the $X_T$-$Y_T$-$Z_T$ co-ordinate frame and $X_d$-$Y_d$-$Z_d$ co-ordinate frame
4. Figure 4: (i) Normalized force $\mathbf{f_{y1}}$ vs normalized displacement $u_{y1}$ for varying tilt angle $\beta$ and $\gamma$ (ii) Normalized $(\mathbf{m_{z1}}-4\theta_{z1})/\mathbf{m_{xd1}}$ vs normalized moment $\mathbf{m_{x1}}$ at $\theta_{y1}=0$ and $\theta_{z1}=0.02$ radians for varying tilt angle $\beta$ (iii) Normalized displacement $u_{x1}$ vs normalized displacement $u_{y1}$ for varying $\beta$ and $\gamma$ (iv) Rotational displacement $\theta_{xd1}$ vs Rotational displacement $\theta_{y1}$ for varying $\gamma$
5. Figure 5: (i) Load stiffening during in-plane translation along y, (ii) In-plane translation along y due to in-plane rotation in the presence of $\mathbf{m_{ys}}$, (iii) In-plane translation along y due to in-plane rotation in the presence of $\mathbf{m_{zs}}$, (iv) Load stiffening during in-plane rotation due to x
6. Figure 6: Parasitic Error motion in $u_{xs}$ due to $u_{ys}$ and $\theta_{xs}$

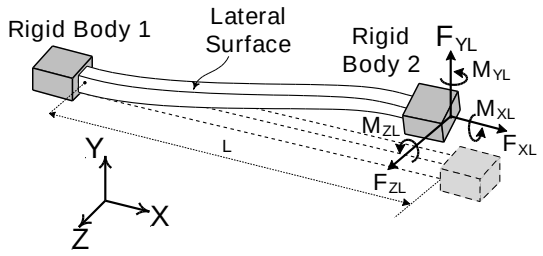
Rigid Body 1
Lateral
Surface
Rigid
Body 2
$F_{YL}$
$M_{YL}$
$M_{XL}$
$M_{ZL}$
$F_{XL}$
$F_{ZL}$
L
Y
X
Z

Figure1.eps

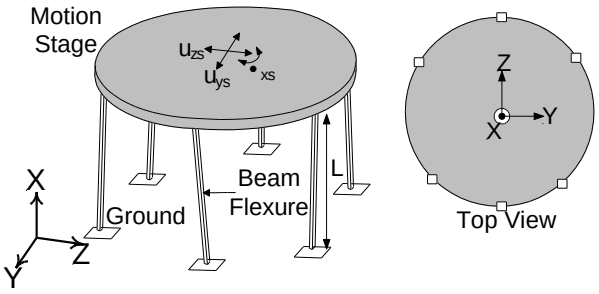
Motion
Stage
$u_{zs}$
$u_{ys}$
$\theta_{xs}$
X
Y
Z
Ground
Beam
Flexure
L
Z
Y
X
Top View

Figure2.eps

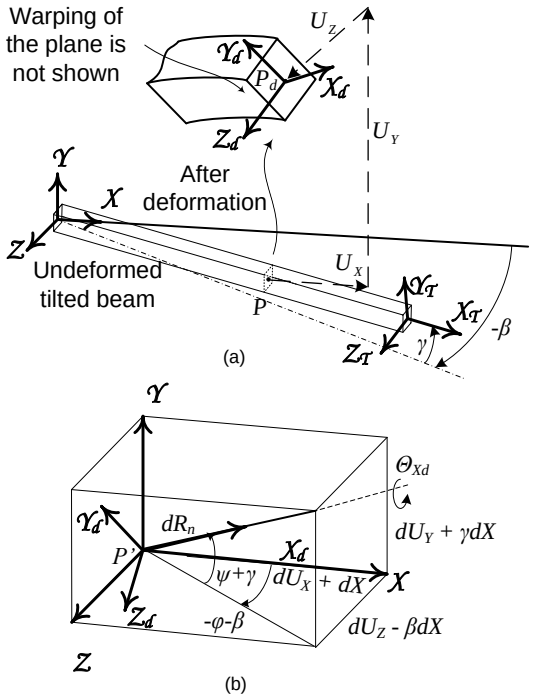
Warping of
the plane is
not shown
$U_Z$
$Y_d$
$P_d$
$X_d$
$Z_d$
$U_Y$
$Y$
$X$
$Z$
After
deformation
Undeformed
tilted beam
$U_X$
P
$Y_T$
$X_T$
$Z_T$
$\gamma$
$-\beta$
(a)
$Y$
$\Theta_{Xd}$
$Y_d$
$dR_n$
$dU_Y + \gamma dX$
P
$X_d$
$\psi+\gamma$
$dU_X + dX$
$X$
$Z_d$
$-\varphi-\beta$
$dU_Z - \beta dX$
$Z$
(b)

figure3.eps

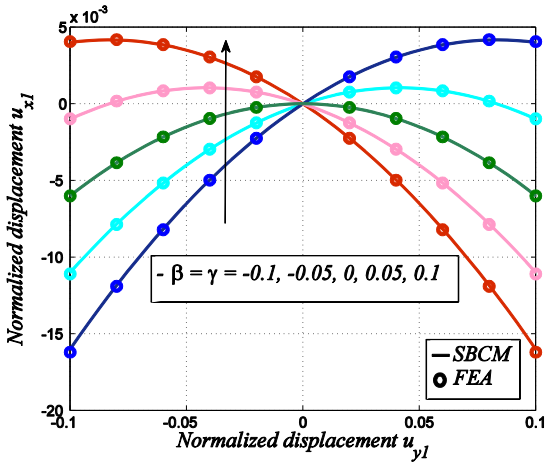


Figure4(i).eps

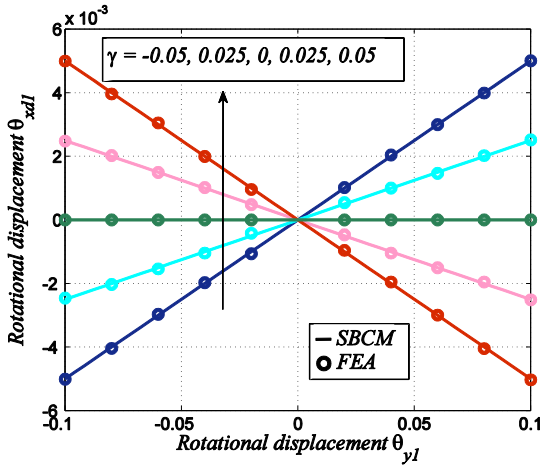


figure4(ii).eps

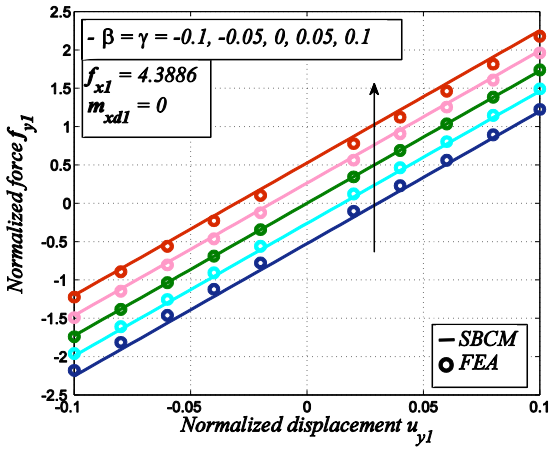


figure4(iii).eps

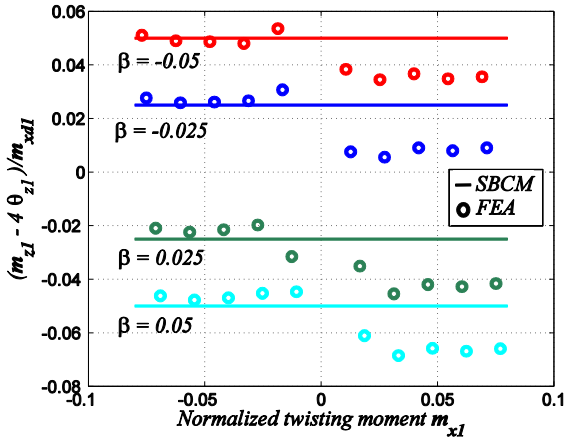


figure4(iv).eps

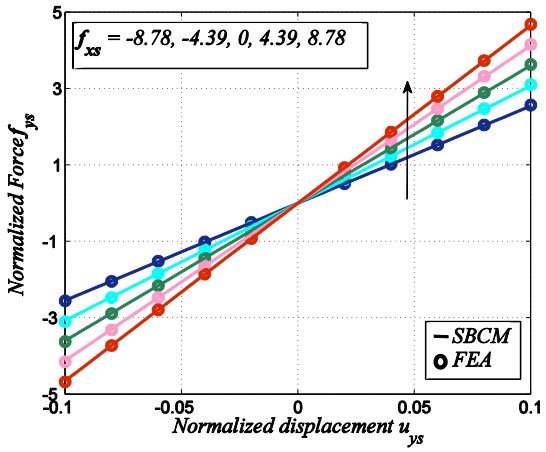


figure5(i).eps

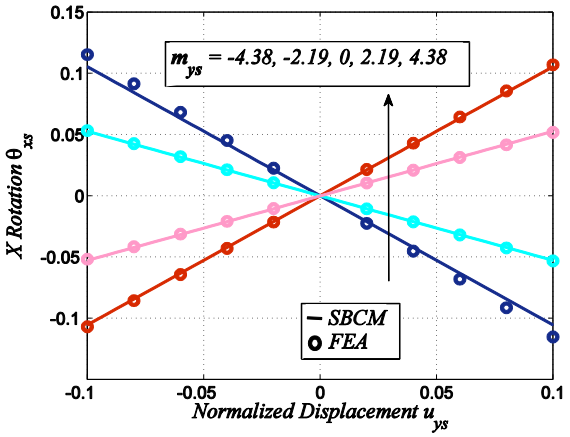


figure5(ii).eps

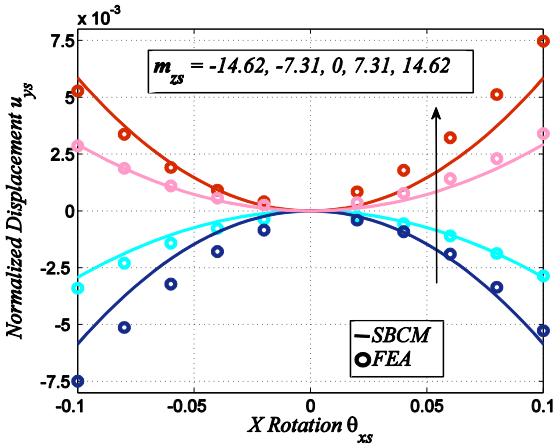


figure5(iii).eps

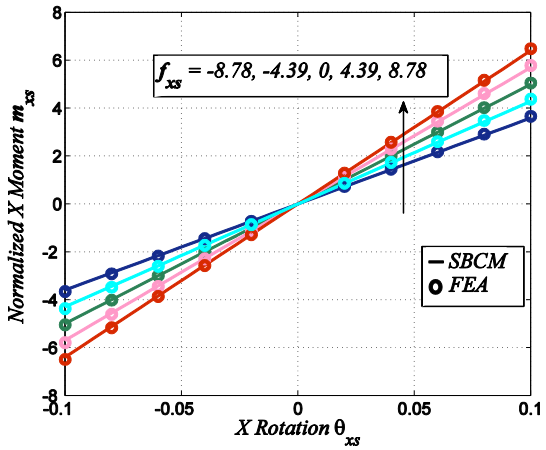


figure5(iv).eps

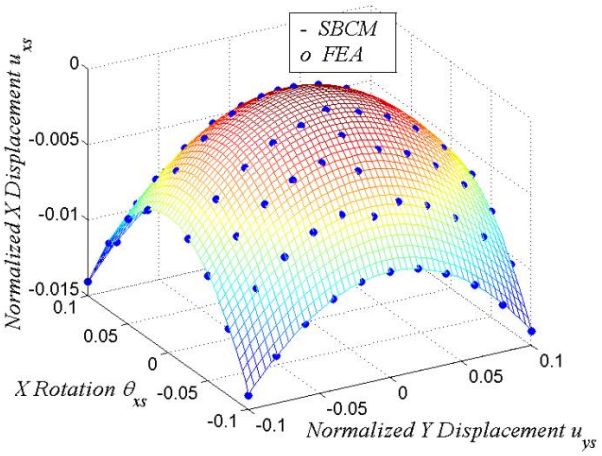


figure6.tiff